Biogeochemistry (2009) 96:25–48
DOI 10.1007/s10533-009-9343-7

The chemical character and behaviour of phosphorus in poorly oxygenated sediments from open sea to organic-rich inner bay in the Baltic Sea

K. Lukkari · M. Leivuori · A. Kotilainen

Received: 25 July 2008 / Accepted: 1 July 2009 / Published online: 22 July 2009

Abstract The chemical composition and vertical distribution of phosphorus (P) in poorly oxygenated sediments in a continuum extending from the open Baltic Sea towards an organic-rich inner bay were characterized by sequential extraction to examine the potential for release of sediment P. The chemical composition of P was related to chemical and physical characteristics of the sediments and the chemistry of pore water and near-bottom water to better understand the behaviour of P. Sediment P increased towards the inner bay, and the concentration of organic matter appeared to dictate its composition: the dominance of apatite-P turned to dominance of organic P (OP). Sediment P burial and, thus, release from sediment P reserves varied depending on the chemical composition of P. Dissolved species at the sediment–water interface suggested fluctuating redox conditions that affect P binding at short time scale. Redox-sensitive, iron (Fe)-bound P was usually relatively low because of poor oxygen (O_2) conditions, which emphasized the role of OP in P release. The results indicate that, over the long term, the abundant organic P reserve may support a significant continuing P release from hypoxic sediments in the severely eutrophied Gulf of Finland (GoF) because capture of P into Fe oxyhydroxides at the sediment surface is restricted. The average long-term minimum annual rate of P release from poorly oxygenated sediments below about 60 m depth in the GoF was approximated on the basis of the vertical distribution of sedimentary P forms and estimates of sedimentation rate.

Keywords Baltic Sea · Fractionation · Organic matter · Phosphorus · Sediment

Present Address:
K. Lukkari (✉) · M. Leivuori
Finnish Institute of Marine Research, Marine Research Centre/Finnish Environment Institute, Erik Palménin aukio 1, P.O. Box 140, 00251 Helsinki, Finland
e-mail: kaarina.lukkari@ymparisto.fi; kaarina.lukkari@fimr.fi

A. Kotilainen
Geological Survey of Finland, P.O. Box 96, 02151 Espoo, Finland

Introduction

Eutrophication is a serious problem in the Baltic Sea, the Gulf of Finland (GoF) being one of the most severely deteriorated areas. Although anthropogenic phosphorus (P) loading to the GoF has decreased during the past decades, intense algal blooms are still common (HELCOM 2003). Partly because of the release or turnover of available P from the sediment (Emeis et al. 2000). According to classical theory, if oxygen (O_2) is depleted in the near-bottom water, the subsequent reduction of iron (Fe) will result in the release of P from Fe oxyhydroxides (Einsele 1936,

1938; Mortimer 1941, 1942). Oxygen depletion is common in the GoF (HELCOM 2003) primarily due to O_2 consumption by the microbial degradation of organic matter (OM), in addition to the poor vertical mixing of the water column. Poor mixing is mainly caused by salinity stratification. Furthermore, the topography of the seafloor allows saline, often hypoxic, bottom water to flow from the Baltic Proper into the GoF (Winterhalter et al. 1981).

In open sea sediments, P originating from terrestrial inputs via riverine transport or produced in the marine systems are deposited after resuspension and transportation. Various biogeochemical processes can transform deposited P into more labile forms (by dissolution and degradation) or more stable forms (by precipitation and incorporation into cells) (Froelich et al. 1982; Boström et al. 1982; Ruttenberg 2005), and P may cycle several times at the sediment–water interface before it is buried with sediment (e.g. Sundby et al. 1992). Fine grained and OM-rich material accumulates in calm sedimentary environments such as deep basins. Metal oxide coatings on small-sized particles, such as clay minerals, adsorb P efficiently, but O_2 depletion can enhance release of this particle-bound P. Phosphorus can also be released from the sediment in oxic conditions, through degradation of organic P (OP) compounds, anion competition, increase in pH, and shortage of sorption sites (Hingston et al. 1967; Boström et al. 1982; Ryden et al. 1987).

The binding form determines whether sediment P can be released to the water column or whether it is buried and removed from the nutrient cycle. Fractionation methods are used to classify sediment P into different pools according to its binding forms and solubility properties. Commonly separated forms are pore-water (or loosely sorbed) P, P bound to oxides of reducible metals (mainly Fe), P bound to oxides of metals not sensitive to chemical reduction (mainly aluminum, Al), calcium (Ca)-bound or apatite-P of detrital or authigenic origin, and OP (labile or refractory forms) (Boström et al. 1982; Van Eck 1982; Pettersson et al. 1988; Ruban et al. 1999).

Although the release of P from sediment depends on its chemical form, studies characterizing P reserves in Baltic Sea sediments are sparse, and comparison of the results is complicated by the use of different methods. Carman and Jonsson (1991) found apatite-P to dominate in most sediment types in western Baltic Proper, though redox-sensitive P was high in oxic sediments in the archipelago and near the shore. Fe-bound P and apatite-P, dominated in southwestern Baltic (Aarhus Bay, Kattegat, and Skagerrak), followed by residual OP, while Al-bound P was abundant near the coast (Jensen and Thamdrup 1993; Jensen et al. 1995). Aigars (2001) reported for the Gulf of Riga that redox-sensitive P dominated in the topmost sediment and inorganic P was higher than OP. In contrast to this, Virtasalo et al. (2005) found that in surface sediments at Archipelago Sea, OP dominated followed by detrital apatite-P, and redox-sensitive P was slightly higher than authigenic apatite-P. Another study in the Archipelago Sea showed high variation in P forms during the development of the sea area after the deglaciation (Virtasalo and Kotilainen 2008). Łukawska-Matuszewska and Bolałek (2008) reported very high and variable P contents in different sediment types in the Gulf of Gdansk, southern Baltic, as well as dominance of OP, followed by Al-bound P.

Studies on chemical character of sediment P in the GoF are very few although it is heavily loaded and one of the most severely eutrophied areas in the Baltic. Carman (1998) reported low redox-dependent P in the hypoxic Baltic Proper and high TP in the eastern GoF but he did not present P fractionation results from the GoF. Lehtoranta (1998) suggested that residual P and Fe–P followed by Al–P dominated in surface sediments at the shallow eastern GoF, while residual P and Al–P dominated (although Al–P may have been overestimated; Chang and Jackson 1957, Williams et al. 1971) near the eastern Finnish coast. However, he did not separate redox-sensitive P. Recently, we explored the chemical character of P in shallow coastal sediments overlain by oxic near-bottom water in the northern GoF and Archipelago Sea and found that the area affected by sediment transportation was dominated by apatite-P. In contrast, OP forms dominated in the eastern coast, where the OM-rich sediments are vulnerable for temporal hypoxia (Lukkari et al. 2009).

The abundance of OP as well as its role in release of P from coastal sediments (Lukkari et al. 2009) suggests that OP may also have significant role in P release from the hypoxic area in the open GoF. Release of sediment P under O_2 depletion is usually explained by dissolution of ferric-iron compounds

(Einsele 1936, 1938; Mortimer 1941, 1942), although O_2 depletion can also enhance release of OP (Ingall et al. 1993; Ingall and Jahnke 1994; Ingall and Clark 1998; Suzumura and Kamatani 1995). This, as well as the common hypoxia in the Baltic, emphasizes the need for studying the effect of the chemical character of P on its release from hypoxic sediments where the amount of Fe–P is smaller. A suitable environment for exploring this phenomenon is one where the concentration and forms of P can be assumed to change, for example, a continuum beginning from open sea and extending to inner bay, towards source of high P loading. In the Baltic, such studies are few. Carman and Jonsson (1991) fractionated P from offshore and near-shore sediments in the western Baltic Proper but concentration of P, especially OP, was low and sediments were mainly oxic. Virtasalo et al. (2005) studied sediment surface layers of different O_2 status in the complex Archipelago Sea but they did not find any significant spatial distribution in P fractions, except higher detrital apatite-P in the inner than the outer Archipelago. Łukawska-Matuszewska and Bolałek (2008) studied sediment P in the Gulf of Gdansk but their study sites were mainly oxic and consisted of a variety of different sediment types, including sandy sediments and dredging areas.

In this study, we investigated the chemical composition and distribution of sediment P along a continuum from the northern Baltic Proper to the organic-rich eastern GoF, characterized by low dissolved O_2 in the near-bottom water. Our objective was to assess the change in the chemical character and, thus, in the potential for release or burial of sediment P from hypoxic open sea area. We paid special attention to avoid oxidation of the reduced sediment samples prior to extraction because oxidation is known to affect their P composition (e.g. Lukkari et al. 2007a). This is often forgotten in sediment P fractionation studies. The chemistry and behaviour of sediment P is dependent on the physico–chemical properties of the sediment. Thus, relationships were sought between the P forms and the chemical and physical characteristics of the sediments and the chemistry of pore water and near-bottom water to obtain a more comprehensive insight into the P chemistry and its behaviour at the sediment–water interface under O_2 depletion.

Materials and methods

Research area and sediment types at the sampling sites

The GoF is a shallow (mean depth 37 m, area 29 571 km^2) non-tidal bay in the eastern Baltic with often stratified, low salinity water (5–10 PSU). The halocline varies at about 60–80 m depth (Kullenberg 1981; Alenius et al. 1998). The seven sampling sites form a west-to-east continuum beginning from the northern Baltic Proper and terminating in the eastern GoF (Fig. 1). Water depth ranged from 58 to 89 m, with the deepest sites in the middle of the GoF (site 4) and the shallowest site in the easternmost location (site 7).

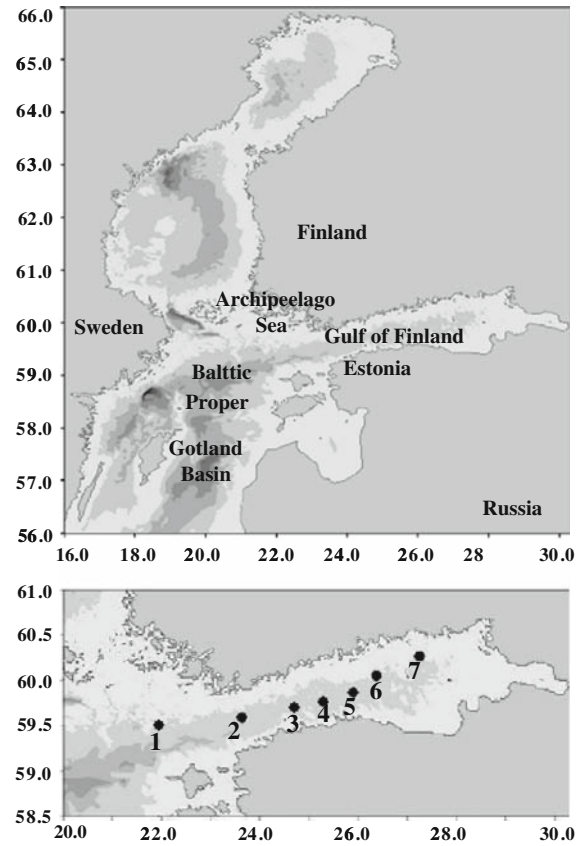

Fig. 1 The research area and location of the sampling sites in the GoF and the northern Baltic Proper, Baltic Sea. The numbers refer to following sampling sites: 1 = AS7; 2 = JML; 3 = GF1; 4 = E3; 5 = GF2F; 6 = LL3a; and 7 = XVI

The basement consists of Paleoproterozoic crystalline bedrock (Koistinen et al. 2001). In most parts of the GoF, till overlays the bedrock. Bedrock or till that is not exposed due to erosion, is often covered by late glacial and postglacial clays, silts, or sand (Winterhalter et al. 1981). Modern sediments in the studied basins are mostly muddy clays rich in Fe and humic matter and poor in Ca-carbonate (Winterhalter et al. 1981; Conley et al. 1997; Carman 1998). In the studied cores, beneath the fluffy surface layer, sediments were usually laminated with grey and black laminae of varying thickness and, at the surface, occasionally embedded with brownish lamina. Traces of bioturbation and disturbed sedimentary units appeared at depth of a few centimeters and deeper in the cores, between laminated units. Water content was 90–95% at the surface, <80% below 5 cm depth, and about 60–70% at 25 cm depth. The sediment surface at sites 1, 4, 5, and 7 had white bacteria growth (or remains of it), and often a strong smell suggested the presence of hydrogen sulfide.

Sampling

Sampling cruises of research vessel (r/v) Aranda took place in September 2003 (sites 1, 2, and 3), in April 2004 (sites 4, 5, and 6), and in August 2004 (site 7). All sampling sites were selected according to surveyed echo sounding data, which was used to estimate sediment depth across sites. Sediment samples for P fractionation and other chemical determinations were taken with a Gemax gravity corer (two acrylic cylinders, diameter 9 cm, length ca. 60 cm). Six cores were recovered per site. In addition, one pair of cores was recovered at two sites located close to site 5. The results of the additional cores, however, are only included in statistical analyses because their P composition was very similar to that determined at site 5, which located within the same sedimentation basin (Lukkari 2008). Two cores were put on a slicing table and covered with a glove bag tightly joined to another glove bag. The glove bags were sealed and filled with nitrogen (N_2, purity 99.5%) until O_2 content was <5–10% (detected with Gas Alert detectors calibrated against fresh air, O_2 content 20–21%). After the near-bottom water (5 cm above the sediment) was sampled and the rest of it removed, the sediment was sectioned into 1-cm segments at every centimeter down to 10 cm, then at every fifth centimeter down to 25 cm depth (except site 5 continuously up to 15 cm and site 7 only up to 15 cm). The samples of two parallel cores were pooled and sealed in plastic containers in the second glove bag (cooled with ice, $O_2 < 5\%$). The containers were vacuum packed (Tecla s.n.c Vacum 33) into gas-tight plastic bags (filled with N_2) and stored at 5°C (in the dark) until analysis.

Analytical methods

Analytical methods used for determinations in the water column, pore water, and sediment samples are described in detail in Lukkari et al. (2008) and they are and introduced only shortly here. A detailed description of the P fractionation procedure is given in Lukkari et al. (2007b).

Water column and pore water samples

Water column salinity, temperature, and dissolved O_2 were determined with a CTD instrument. Dissolved P (PO_4–P, i.e. PO_4^{3-}), N as nitrate (NO_3–N, i.e. NO_3^-) and ammonium (NH_4–N, i.e. NH_4^+), silicate (SiO_4–Si), and total P (TP) and N (TN) were determined onboard with an autoanalyser by methods described in Hansen and Koroleff (1999). Dissolved O_2 in the near-bottom water (ca. 5 cm above the sediment) was determined by Winkler titration (Grasshoff 1983). The near-bottom water was also analysed for dissolved P and N (filtered, pore size 0.4 μm) and total P and N (unfiltered) as above. Sediment P flux (incubation-derived) was estimated by calculating the difference in PO_4–P at 0 and at 5 h after incubation over the surface area of replicate cores.

Pore water in the surface sediment (up to ca. 4 cm depth) was collected in argon (Ar) atmosphere (atm) using a whole-core hydraulic squeezer (Bender et al. 1987; Mäkelä and Tuominen 2003) and analysed onboard for the dissolved nutrients. In addition, pore water was separated from deep sediment profiles (except from sites 1, 2, and 3) by centrifuging 1-cm sections of sediment (same depth intervals as above, sample handling and filtration under N_2-atm). A portion of the pore water samples was analysed for total dissolved Fe and manganese (Mn) by inductively coupled plasma atomic emission spectroscopy (ICP-AES, TJA-25, Thermo Jarrell Ash). Detection

limits for Fe and Mn were 0.8 and 0.3 μmol l^{-1} and recovery was 113% for both metals.

Sediment

Two sediment cores were sectioned (at the same intervals, without N_2 atm), immediately frozen (−18°C), and later freeze-dried and homogenized for analysis of total P (TP_{sed}), Fe, Mn, Al, and Ca. The elements were measured with an ICP-AES after digestion (fluoric acid/aqua regia/boric acid; Loring and Rantala 1992, as modified by Leivuori 2000). In the reference materials, the recovery of P was 110% and that of Ca, Fe, Mn, and Al from 96% to 110%. Detection limits for total P, Fe, Mn, Al, and Ca were 0.5, 0.4, 0.1, 0.4, and 1.3 μmol g^{-1}, respectively.

Redox potential, pH, and temperature were determined from one core with electrodes. Measurements were made at every 1-cm interval from 5 cm above the sediment down to ca. 10 cm depth within the core. In this study the redox potentials determined are considered descriptive only (Stumm and Morgan 1996; Drever 2002). Most of the sediments were anoxic and may contain hydrogen sulfide deleterious for common electrodes.

^{137}Cs activity was determined at the Finnish Radiation and Nuclear Safety Authority (according to Kyzyurov et al. 1994; Kankaanpää et al. 1997; Mattila et al. 2006) for sediment dating and estimation of sediment accumulation rate (SAR). ^{137}Cs peak values in the GoF indicate sediment deposition in 1986 (fallout after the Chernobyl accident). SAR values for sites 1, 2, and 3 are from Mattila et al. (2006), while those for the other sites were estimated at the Geological Survey of Finland (GTK). Particle size distribution was determined at GTK by sieving and with a Sedigraph analyser. Sediment total carbon (TC_{sed}), nitrogen (TN_{sed}), and sulfur (TS_{sed}) were determined with a LECO CNS-2000 analyser at the Pirkanmaa Regional Environment Centre.

P fractionation

The P fractionation (Table 1) was carried out mainly following the scheme of Jensen and Thamdrup (1993), a modification of the method proposed by Psenner et al. (1984). In this study, the scheme was further modified (Lukkari et al. 2007b). Briefly, in step I, NaCl separates loosely bound and pore water P (referred to later as NaCl-iP). In step II, NaBD fractionates redox-sensitive P bound to hydrated oxides of reducible metals, mainly Fe (NaBD-iP). In step III, NaOH extracts P bound to hydrated oxides of Al and other metals not reduced in the previous step (NaOH-iP) and labile OP (NRP). In step IV, HCl dissolves Ca-bound P, mainly from apatite minerals (HCl-iP). In step V, the dried and combusted sediment residues are extracted with HCl to separate residual P, i.e., refractory OP (Res-P). Steps I–II were carried out under N_2-atm to avoid oxidation of the sediment. Extracts were analysed for PO_4–P (filtered) and TP (unfiltered) (Koroleff 1983). The extracts in steps II and III were also analysed for total dissolved (T_{diss}) Fe, Mn, Al, Ca, magnesium (Mg), and Si by ICP-OES at the Institute for Environmental Research (University of Jyväskylä). Detection limits were 10 mg l^{-1} for Fe, Mn, and Al and 20 mg l^{-1} for Ca, Mg, and Si.

The P fractions can be roughly divided into reactive (NaCl-iP, NaBD-iP, and NRP) and immobile (NaOH-iP, HCl-iP, and Res-P) sediment P. Burial fluxes for P were calculated by multiplying the

Table 1 Outline of the P fractionation scheme

Step	Extractant	Separated P fraction
I	0.46 M sodium chloride (NaCl), 1 h	Pore water P, loosely sorbed P (NaCl-iP)
II	0.11 M sodium dithionite in sodium bicarbonate (NaBD), 1 h	P bound to oxides of reducible metals (Fe and Mn) (NaBD-iP)
III	0.1 M sodium hydroxide (NaOH), 18 h	P from Al oxides, non-reducible Fe-compounds (NaOH-iP) and labile organic P (NRP)
IV	0.5 M hydrochloric acid (HCl), 1 h	Apatite and other inorganic P (HCl-iP)
	Ignition of the sediment residue: 2 h at 550°C	
V	1 M hydrochloric acid (HCl), 16 h	Residual, mainly refractory organic P (Res-P)

immobile P in the surface layer by the SAR values. The burial efficiency of sediment total P was expressed as the portion of immobile P in the surface layer as percentage of the total extractable P (TP_{extr}), i.e., the sum of P in the separate fractions (Jensen et al. 1995; Lukkari et al. 2008). Thus, the burial efficiency of P here is not the same as the burial efficiency of reactive P. The long-term average of minimum annual efflux of sediment P was calculated from the concentration difference between reactive P in the surface layer and at the nearest sample depth to the ^{137}Cs maximum (i.e., year 1986) at each site, and dividing that by the age difference (in years).

Statistical analyses

Statistical analyses were carried out using the mixed model, run with the Statistical Analysis Software program (SAS Systems for Windows, 8.02, SAS Institute Inc.) to determine which variables (elements in sediments and extracts) explain the P fractions. The mixed model was chosen because the observations were correlated. The sampling site was set as a random variable, and the sediment depth layer was treated as a repeated factor (autoregressive structure in the longitudal data assumed). The dependence was tested with the *F*-test (significant when ≤ 0.050). Parameters for the mixed model were chosen on the basis of their mutual relationships, determined using a Pearson correlation analysis with Bonferroni probabilities and a principle component analysis.

Results

Water column and pore water

The chemistry of the near-bottom water and the pore water varied among the sites (Table 2). Salinity was lowest at the eastern end (site 7) and highest in the central GoF. Sites 7 and 6 were barely oxic, while the other sites were hypoxic ($O_2 < 2.0$ ml l^{-1}), particularly those in the central GoF. PO_4–P showed an opposite trend than O_2, being highest at site 3 and lowest at site 7. SiO_4–Si was also highest at site 3. The incubation-derived PO_4–P flux was negative, i.e., with respect to sediment, at sites 2 and 6, while it was positive at the rest of the sites (up to 1,774 μmol m^{-2} day^{-1} at site 7). Similar to measured O_2 concentrations, NO_3–N was highest at site 7 and lowest at site 3. NH_4–N and dissolved Mn were both highest at site 4 and lowest at site 6. Fe_{diss} was relatively low and under detection limit at the westernmost site (1).

Table 2 Parameters describing properties of the sampling sites and near-bottom waters

Parameter	Site 1	Site 2	Site 3	Site 4	Site 5	Site 6	Site 7
Water depth (m)	71	79	83	89	84	63	58
Near-bottom water							
O_2 (ml l^{-1})	1.6	1.8	0	0.4	0.8	2.4	2.5
PO_4–P (μmol l^{-1})	3.4	3.9	5.2	3.8	3.3	3.1	2.8
TP (μmol l^{-1})	2.8	4.0	7.6	3.5	3.4	3.7	5.6
SiO_4–Si (μmol l^{-1})	48.7	44.9	53.8	53.4	48.7	40.1	43.5
NO_3–N (μmol l^{-1})	5.5	3.6	0.4	1.6	6.9	10.4	11.6
NH_4–N (μmol l^{-1})	5.8	2.5	6.6	8.3	2.5	0.8	5.1
TN (μmol l^{-1})	28.7	19.7	32.0	10.3	27.5	29.7	43.7
PO_4–P flux (μmol m^{-2} day^{-1})	198	−209	1,370	207	357	−245	1,774
Fe_{diss} (μmol l^{-1})	0	0.5	0.2	0.9	0.5	0.8	1.2
Mn_{diss} (μmol l^{-1})	2.2	4.3	12.2	16.6	2.4	1.6	13.9
Salinity (PSU)	8.6[a]	8.2[a]	8.5[a]	9.7[a]	9.5[a]	8.2[a]	7.0[a]
Temperature (°C)	3.5[a]	3.5[a]	3.8[a]	5.1[a]	4.9[a]	3.9[a]	2.6[a]
pH	7.3	6.7	7.0	6.5	7.8	–	6.9
E_h (mV)	176	293	74	383	435	375	149

[a] Values were determined ca. 1 m above the sediment

The concentrations of dissolved elements usually increased with depth at the sediment–water interface (except for NO_3–N; Fig. 2). Pore water NO_3–N was not detectable at site 7 and it was highest at site 5. Pore-water PO_4–P was lowest at site 6 and highest at sites 1 and 3 (up to 146 μmol l^{-1}). SiO_4–Si (maximum 765 μmol l^{-1}) followed the same pattern. NH_4–N was lowest at site 7 and highest at site 3. Pore-water Mn_{diss} was approximately ten times higher than Fe_{diss} and it was more or less uniform with depth at the three westernmost sites.

Deep pore water profiles (no data from sites 1, 2, and 3) showed that increase in PO_4–P with sediment depth usually continued below the surface layers (Fig. 3b). Over the whole depth profile PO_4–P was lowest at site 4 and highest at site 6 (maximum 243 μmol l^{-1}). As at the sediment–water interface, Mn_{diss} was clearly higher than Fe_{diss} in the deep pore water profiles. It generally decreased with depth, while Fe_{diss} did not show clear trends with depth.

Sediments

The elemental composition of the sediments changed with depth and from west to east (Fig. 4; Table 3). TP_{sed} generally decreased with depth, the drop being sharp just below the surface layer. It ranged from 25.7 to 91.9 μmol g^{-1} DW and was highest at the two easternmost sites and lowest at site 3. TC_{sed}

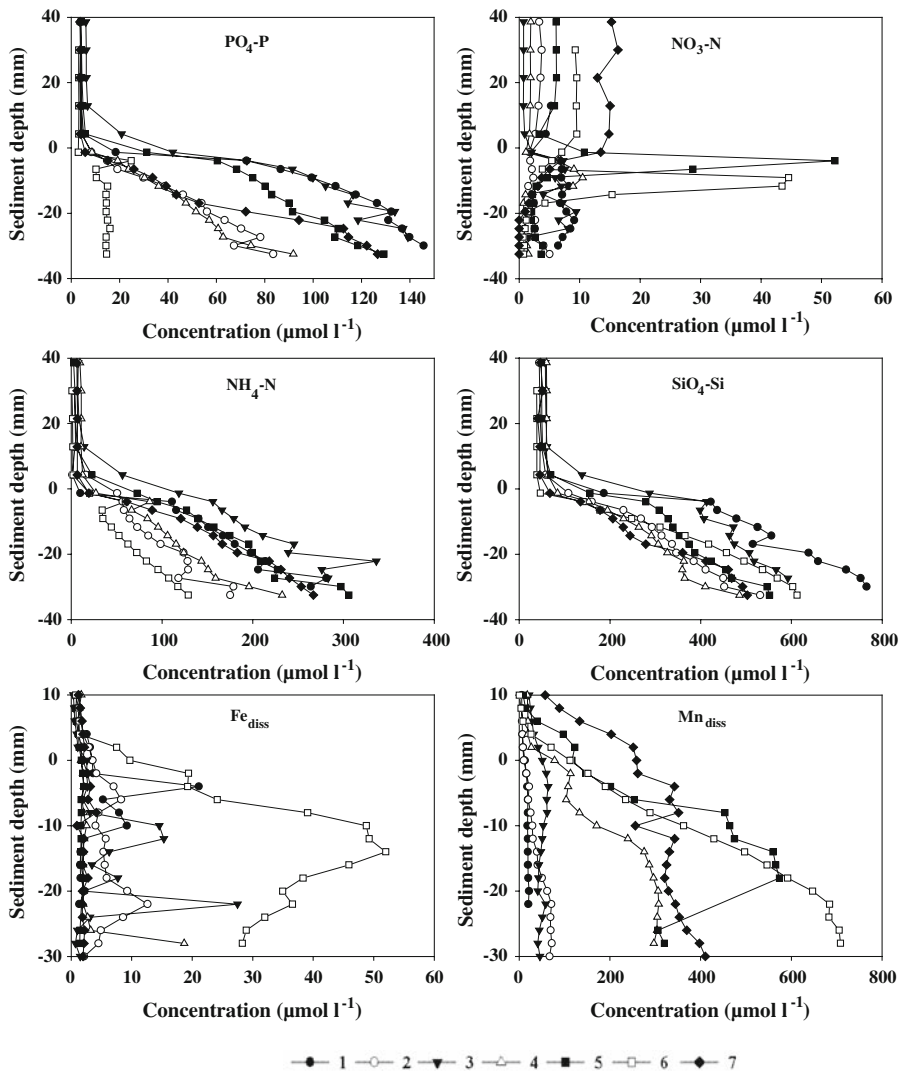

Fig. 2 Dissolved PO_4–P, NO_3–N, NH_4–N, Fe, and Mn in the pore water in surface sediments. The *y*-axis represents sediment depth in cm and the *x*-axis represents concentration in μmol l^{-1}

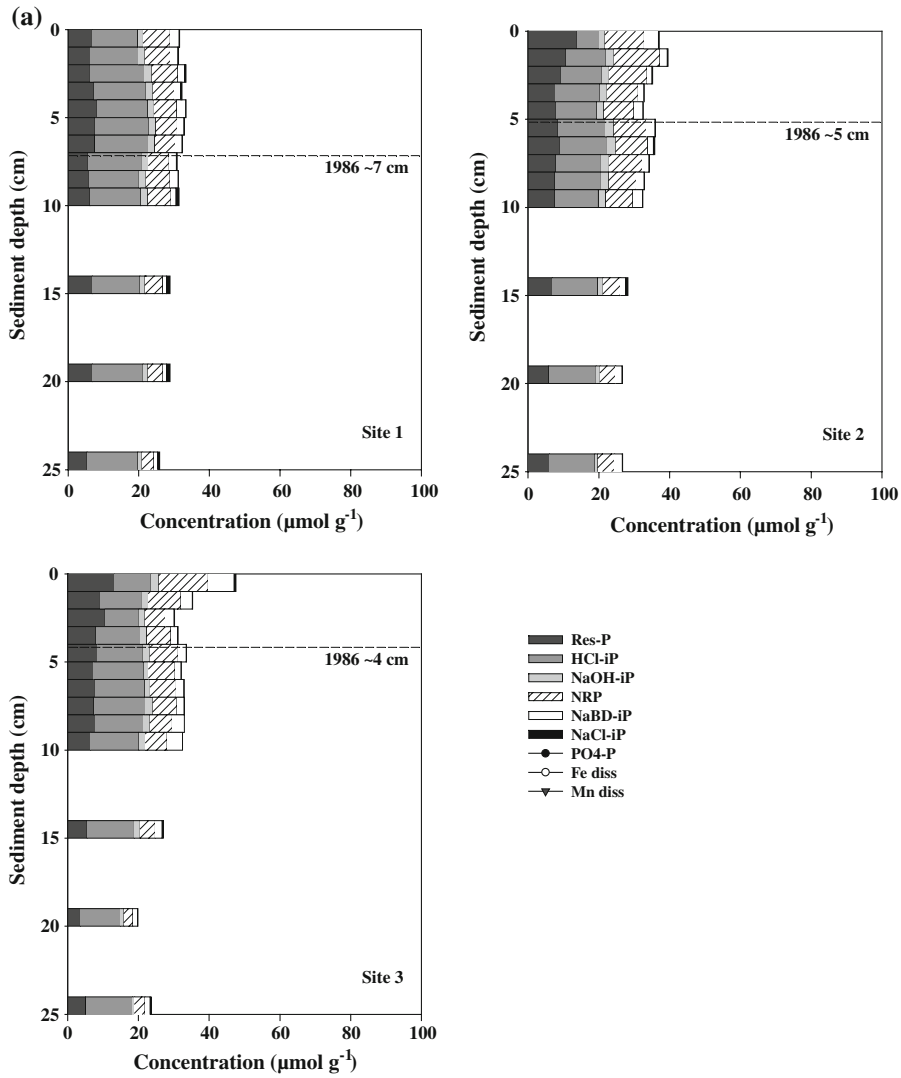

Fig. 3 **a** The vertical distribution of P fractions in sediments at sites 1, 2, and 3. The *y*-axis represents sediment depth in cm (0 is the sediment surface) and the *x*-axis represents concentration of P fractions in μmol g^{-1} DW. Differences between triplicate or duplicate samples (including the samples from the sites in **b**) were <1.2, <1.2, <1.6, <1.7, and <1.5 μmol P g^{-1} DW for fractions NaCl-iP, NaBD-iP, NaOH-iP, HCl-iP, and Res-P, respectively. The *dashed lines* (**a**, **b**) show the approximate depth of the ^{137}Cs maxima (i.e., year 1986). **b** Dissolved PO_4–P, Fe, and Mn in the deep sediment pore water and the vertical distribution of P fractions in sediments at sites 4, 5, 6, and 7. The *y*-axis represents sediment depth in cm (0 is the sediment surface). The *x* on top represents concentration of pore water elements in μmol l^{-1} and the *x*-axis below represents concentration of P fractions in μmol g^{-1} DW

(range 1,468–10 457 μmol g^{-1} DW) and TN_{sed} (120–985 μmol g^{-1} DW) also decreased with sediment depth, and they were highest at the eastern end and lowest at the western end of the transect. Within the sampling area, TC is similar to total organic carbon (TOC). As an example, TOC comprised 94–97% of TC at sites 1 and 2. TS_{sed} did not show any clear trends.

The depth profile of TFe_{sed} was variable (Table 3). Peak concentration (2,049 μmol g^{-1} DW) was in the topmost 1-cm section at site 5, below which it decreased sharply. TFe_{sed} was lowest at site 3. TMn_{sed} was highest (381 μmol g^{-1} DW) at the surface in the central GoF and lowest at sites 1, 2, and 3. In general, TAl_{sed} increased with sediment depth. It was lowest in the topmost layer at site 7 and highest (3,899 μmol g^{-1} DW) in the deepest layer at site 4. TCa_{sed} (maximum 707 μmol g^{-1} DW) was two to three times as high in the topmost 2-cm layer at site 5 as in other samples.

Of the other sediment variables, redox potential varied between 74 and 435 mV in the near-bottom water and between 381 and −196 mV in the sediment, where it decreased sharply within the uppermost 1–2 cm (Fig. 5). It was highest at the surface at site 4 and lowest in deep layers at site 3. The pH ranged from 6.7 to 7.8 in the near-bottom water and in the sediment (Fig. 5). In general, pH increased within 2–3 cm depth, below which it was constant or increased. pH was lowest at the mouth of the GoF

Fig. 3 continued

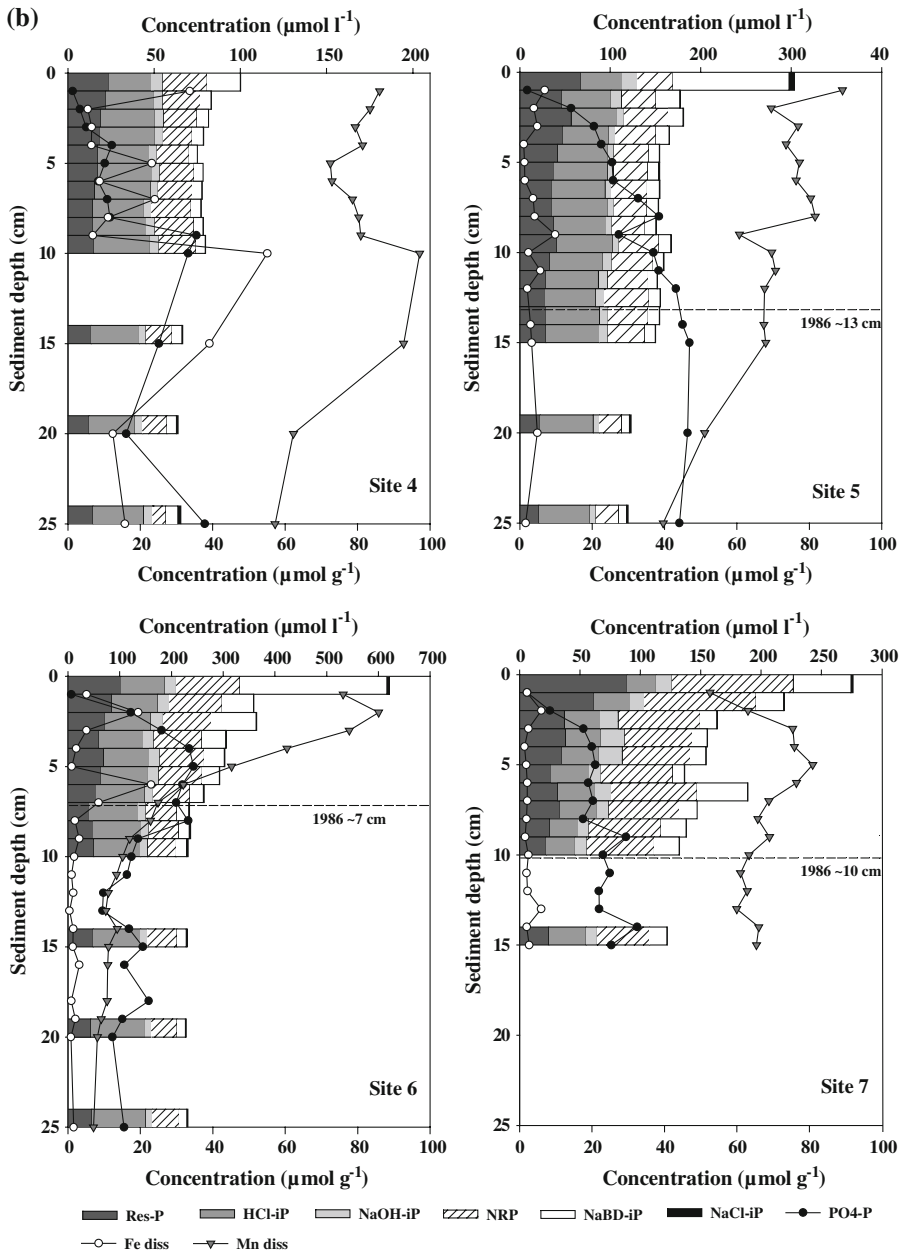

and highest in the central part. Particle size distribution was determined at sites 1, 2, 5, and 6. The clay size-fraction (<2 µm) dominated in the surface sediments (59–77%) and clay content was higher at sites 1 and 2 than at sites 5 and 6.

P fractions

The change in sediment P chemistry from open sea to the organic-rich inner bay was clear (Fig. 3a, b). At most of the sites, especially in the east, TP_{extr} (range 19.9–91.9 µmol g^{-1} DW) decreased with sediment depth. OP (i.e., NRP and Res-P) comprised 31–70% of TP_{extr}, being highest at site 7 and lowest at site 3, while inorganic P exhibited the opposite pattern. Immobile P ranged from 15.9 to 42.2 µmol g^{-1} DW, and reactive P from 4.0 to 58.7 µmol g^{-1} DW.

Apatite-P (HCl-iP) was the dominating P fraction in most profiles, and it tended to increase slightly with sediment depth. It ranged from 6.4 to

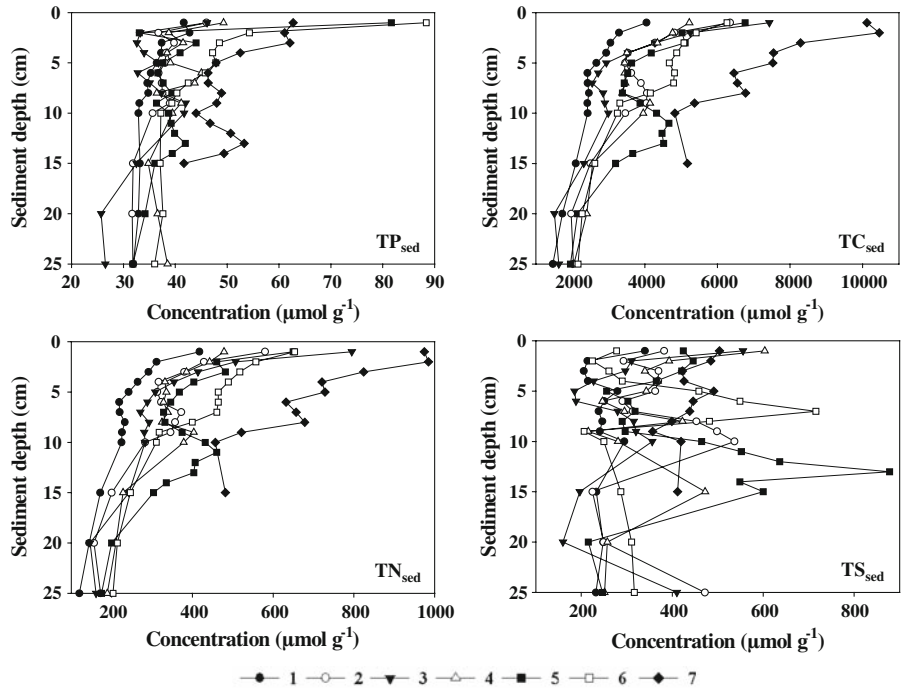

Fig. 4 Total concentrations of P, C, N, and S in the sediment depth profiles. The *y*-axis represents sediment depth in cm (0 is the sediment surface). The *x*-axis represents element concentration in µmol g^{-1} DW

15.6 µmol g^{-1} DW (9–57% of TP_{extr}) and showed a decreasing trend from west to east. At the easternmost site 7, the most abundant P form was NRP. At all sites, it made up 12–44% of TP_{extr} (range 2.5–33.5 µmol g^{-1} DW) and decreased with sediment depth. Usually, Res-P (range 3.6–29.7 µmol g^{-1} DW, 17–38% of TP_{extr}) was the third most abundant P form. This fraction, also, decreased with sediment depth (except at site 1). Similarly to NRP, Res-P increased eastwards. The NaBD-iP fraction (range 1.1–40.6 µmol g^{-1} DW, 4–46% of TP_{extr}) peaked at the sediment surface; below this it decreased sharply but was still present in the deep layers. The central sites 5 and 6 were highest in NaBD-iP, while the westernmost sites were the poorest. NaOH-iP (3–13% of TP_{extr}) was fairly uniform both vertically and spatially. It was highest at the site nearest to the shore (site 7; 6.5 µmol g^{-1} DW). NaCl-iP was present only in small amount (portions of 2–4% of TP_{extr} at maximum). Three of the P fractions and several other parameters determined in the surface sediments showed west-to-east trends in the sampling area (Fig. 6).

Sedimentation of TP_{extr} was lowest at the mouth of the GoF (site 2) and highest in the central basin (site 5). The long-term average of minimum annual P efflux was also highest at site 5 and it was lower in the three westernmost sites than in the two easternmost sites (Table 4). The distribution was not that clear for the burial of P, the burial efficiency of total P, as well as for the SAR. The SAR values varied among the sites (no SAR value for site 4), but with the sedimentation highest in the central basin (site 5). This site also had the highest deposition, burial, and efflux of P. However, burial efficiency was highest and, thus, the efflux of P lowest at sites 1 and 2.

Total elements in extracts

Some of the elements extracted in NaBD and NaOH showed spatial or vertical trends (Table 5). NaBD-extractable Fe decreased with depth. NaOH-Fe also decreased with depth at the easternmost site 7. Overall, site 7 was highest in extracted Fe, while the westernmost sites 2 and 1 were lowest. Al was mostly extracted in NaOH and sites 7, 4, and 1 were high in Al, while site 3 was low. Mn was low in NaOH, but relatively high in NaBD at surface sediments. The alkaline earth metals, Ca and Mg, were low in both extracts and decreased with depth.

Table 3 Total concentrations of Fe, Mn, Al, and Ca in the sediment depth profiles

cm	Site 1				Site 2				Site 3				Site 4			
	Fe	Mn	Al	Ca	Fe	Mn	Al	Ca	Fe	Mn	Al	Ca	Fe	Mn	Al	Ca
1	833	9.9	2,408	316	635	12.6	1,929	262	691	8.1	2,293	270	1,107	116	2,532	285
2	816	9.5	2,932	315	718	9.7	2,659	213	677	9.4	2,712	265	834	14.8	2,371	221
3	747	9.9	2,723	295	824	10.0	2,633	203	674	9.0	2,836	211	911	15.9	2,878	243
4	789	10.4	2,676	296	893	11.0	2,424	204	706	10.1	2,430	213	940	18.2	2,977	238
5	883	11.2	2,942	295	909	11.9	2,558	214	752	11.7	2,699	233	892	18.4	2,750	232
6	812	11.1	3,046	291	835	12.0	3,107	216	733	10.6	3,010	219	985	27.1	3,371	279
7	812	10.8	2,698	251	844	11.2	2,706	198	872	13.0	2,888	225	799	19.8	2,988	235
8	921	11.0	3,001	313	891	12.0	3,150	210	790	12.4	2,906	234	734	22.5	2,902	210
9	792	11.0	2,691	279	909	11.9	3,157	200	860	12.1	3,100	216	658	16.4	3,048	195
10	758	10.9	2,704	279	966	12.7	3,220	209	775	11.8	2,994	230	754	17.6	3,114	246
15	900	11.3	3,212	276	840	11.9	3,179	207	727	12.3	2,967	230	1,033	24.7	3,256	228
20	887	11.7	3,510	284	881	12.2	3,056	262	648	11.0	2,553	283	1,349	23.5	3,416	263
25	1,036	10.8	3,343	289	966	12.4	3,131	243	701	12.6	2,904	285	1,589	25.7	3,899	385

cm	Site 5				Site 6				Site 7			
	Fe	Mn	Al	Ca	Fe	Mn	Al	Ca	Fe	Mn	Al	Ca
1	2,049	381	2,550	443	821	82.5	2,462	234	634	16.0	1,810	209
2	847	235	2,865	707	828	27.0	3,004	293	741	17.9	2,053	213
3	853	25.8	3,065	223	790	27.4	2,694	245	851	19.5	2,485	231
4	839	25.2	3,108	259	802	25.6	2,610	259	763	21.4	2,409	219
5	645	21.4	3,324	203	931	24.1	2,741	250	880	22.5	2,052	214
6	656	21.4	3,313	217	936	20.7	2,670	239	793	23.8	2,426	224
7	837	24.5	3,175	251	952	18.8	2,477	228	845	23.4	2,542	215
8	951	24.9	3,098	267	841	18.0	3,165	229	1,088	28.5	2,941	279
9	790	20.1	3,164	217	782	16.8	3,510	244	858	23.2	2,923	227
10	778	20.8	3,105	226	781	16.3	3,046	243	908	35.2	3,029	242
11	1,126	20.3	2,823	202	–	–	–	–	866	28.5	2,648	212
12	853	22.2	2,534	228	–	–	–	–	858	28.3	2,599	217
13	1,155	114	2,376	261	–	–	–	–	887	28.2	2,829	241
14	927	23.1	2,657	237	–	–	–	–	917	23.8	2,926	224
15	955	20.1	2,532	216	822	16.2	3,174	258	939	21.0	2,943	202
20	762	19.6	3,113	268	886	15.9	3,636	270	–	–	–	–
25	827	19.6	3,173	254	839	14.5	2,769	256	–	–	–	–

The concentrations are presented in μmol g^{-1} DW

Si was higher in NaOH (maximum 1,509 μmol g^{-1} DW) than in NaBD. Values of NaBD-Si generally decreased with sediment depth. Site 7 was highest in NaOH-extractable Si, while site 1 was lowest.

Statistical analyses

For the mixed model analysis, the results obtained from different depth layers were pooled into five age classes (on the basis of the ^{137}Cs dating and assuming constant sediment accumulation over time) because the age of the sediment layers varied among the sites. P fractions (except NaCl-iP) were usually related to these age classes, i.e., time. Sediment TP_{extr} and OP were also related to time. The mixed model analysis revealed also some other statistically significant correlations between P fractions, sediment variables, and elements in extracts (Table 6).

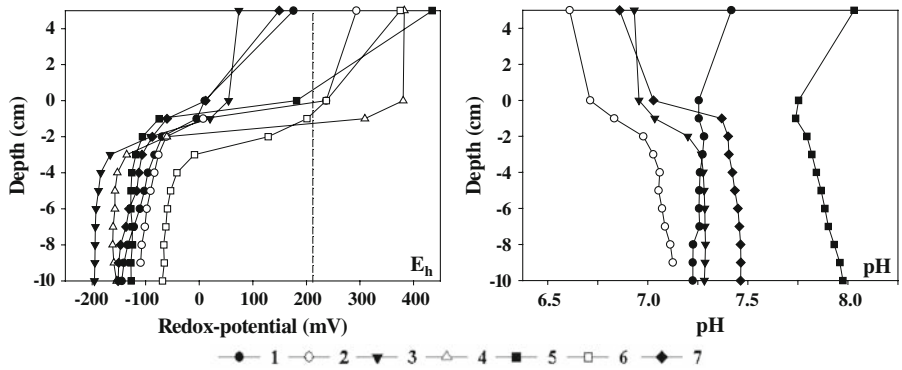

Fig. 5 Redox potential and pH in the near-bottom water and at the sediment surface. The *y*-axis represents sediment depth in cm (0 is the sediment surface, negative values are in the sediment). The *x*-axis represents E_h in mV or pH. The dotted line in the E_h figure represents +230 mV

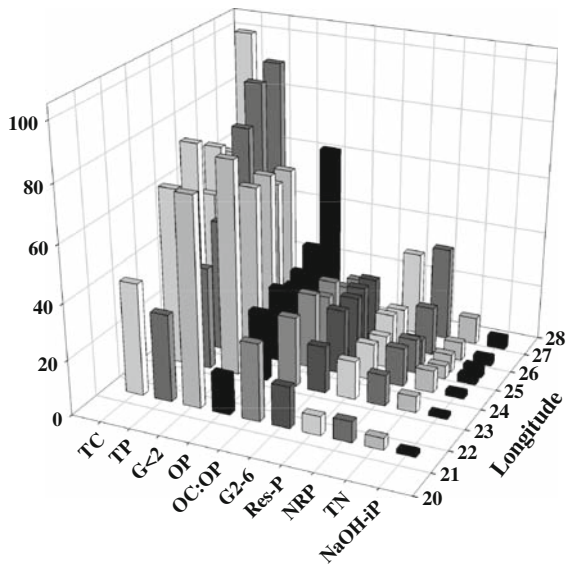

Fig. 6 West-to-east trends of selected sediment parameters in the topmost 1-cm layer. These parameters had $R^2 > 0.5$ when plotted against the latitude of the site. Unit for TP, OP, Res-P, NRP, and NaOH-iP is μmol g^{-1} DW, while that for TC and TN is $\times 10^{-2}$ μmol g^{-1} DW. OC:OP ratios are presented as $\times 10^{-1}$ and grain size classes <2 μm ($G < 2$) and 2–6 μm (G2-6) are presented as %

Discussion

Sediment properties

A closer look at the sediment properties helps to understand the P fractionation results and the behaviour of P. Sedimentation rate was reflected in the accumulation of P: the central GoF received the highest, and the mouth of the Gulf the lowest amount of P per surface area annually (Table 4). The sediment OM content, which increased from west to east, towards the largest river (River Neva), seemed to dictate many properties of the sediment surface (Fig. 6). Sampling season (spring and autumn) may have affected TC_{sed} at the surface, but the eastward increasing trend was clear. TN_{sed} and TP_{sed} mainly followed this same trend, reflecting the increasing OM content (Figs. 4, 6). Kemp (1971) and Williams et al. (1976) found a similar close correlation between OC and both TN and OP in surface sediments of the Great Lakes. In the GoF, OP dominated over inorganic P at the eastern end of the transect (site 7), closest to the heavy P loading, while the opposite pattern was seen at the western end (site 1). Similar clear increasing trend of OP from open sea to inner bay was not reported from the Archipelago Sea (Virtasalo et al. 2005) or the Gulf of Gdansk (Łukawska-Matuszewska and Bolałek 2008). While OP dominated in the eastern GoF, Carman (1998) reported that, inorganic P dominates in sediments of the Baltic. However, Edlund and Carman (2001) found also a relatively high portion of OP of TP in the Baltic Proper, mainly at the anoxic sites.

Iron, Al, Ca, and Mn participate in binding of P. Concentrations of these elements (especially those of Mn, Fe, and Ca) were generally highest in the central GoF (Table 3). In part, this may be due to inflow of near-bottom water from Baltic Proper (Perttilä et al. 1995) and the transport of dissolved and particle-bound elements. The fact that salinity was highest in the central GoF supports this conclusion. Furthermore, Neretin et al. (2003) found Mn-rich amorphous particles associated with OM, Fe, and Ca above the reduced water layer in the Gotland Basin. Ingri et al. (1991) suggested that when high Mn_{diss} in the anoxic water zone reaches oxic zones in the Baltic Proper, P will be scavenged by the formation of Mn-rich particles (see Carman 1998). Despite the hypoxia in

Table 4 Sediment accumulation rates (SAR), sedimentation of P, burial fluxes of P, long-term average for minimum annual P efflux, and burial efficiency of total P at different sites

Site	SAR g m^{-2} $year^{-1}$	Sedimentation of P		Burial of P		Long-term average min. P efflux		Burial effic. (%)
		mmol m^{-2} $year^{-1}$	mg m^{-2} $year^{-1}$	mmol m^{-2} $year^{-1}$	mg m^{-2} $year^{-1}$	mmol m^{-2} $year^{-1}$	mg m^{-2} $year^{-1}$	
1	840[a]	26.5	820	24.5	760	0.12	3.6	93
2	170[a]	6.3	195	5.6	173	0.04	1.3	89
3	350[a]	16.6	515	12.1	376	0.26	8.2	73
5	958	72.7	2,252	46.0	1,424	1.49	46.0	63
6	329	29.2	904	14.5	449	0.82	25.3	50
7	330	30.3	939	22.3	691	0.44	13.8	74

[a] SAR values are from Mattila et al. (2006)

the central GoF, NO_3–N was present in the near-bottom water (Table 2), and probably inhibited the dissolution of Fe (Mortimer 1941, 1971; Froelich et al. 1979). Another explanation for the high Fe, Mn, and P concentrations at the surface in the central basin is transport of resuspended fine particles and OM from the surrounding area in the deepest basins. Fine particles have large surface area for sorption reactions and OM can form OM-metal-P complexes (Schnitzer 1969; Sholkovitz 1976). The high alkali-soluble Fe at the OM-rich easternmost site (Table 5) suggests that part of the TFe_{sed} was bound to OM. In estuaries, mixing of fresh and saline water increases the flocculation of particulate matter (Eckert and Sholkovitz 1976; Sholkovitz 1976). Similarly, the flocculation may be enhanced when depositing material reaches the bottom water of higher salinity.

The decrease in TC_{sed} and TN_{sed} (and partly TP_{sed}) with sediment depth reflects mineralization of the easily degradable OM, and burial of the refractory or slowly degradable compounds (e.g. Kemp 1971). Similarly, the decrease of TS_{sed} below the sediment surface (Fig. 4) suggests that part of the S originated in OM (Jørgensen 1977; Smith and Klug 1981). In coastal marine sediments, S in organic molecules tends to rapidly degrade into sulfide and incorporate into pyrite (Berner 1970; Jørgensen 1977). The black (laminated) sediment surface at most of our sampling sites indicated the presence of some sulfide phases of ferrous iron (Fe^{2+}) (Berner 1970; Mortimer 1971). Furthermore, the black lamina in deeper sediment layers (sometimes coinciding with TS_{sed} peak values) imply reduced P-binding ability, because Fe precipitated with sulfide is unable to diffuse upwards and form oxyhydroxides, which are capable of retaining P, if the sediment surface is oxidized (Mortimer 1971; Krom and Berner 1980; Caraco et al. 1989; Anschutz et al. 1998). At four sites, white bacterial growth on top of the sediment was probably sulfide-oxidizing bacteria (*Beggiatoa* sp., Jørgensen 1977), often found in the GoF (Vallius 2006; Kotilainen et al. 2007), reflecting poor O_2 conditions. The elevated sediment pH in the central basin may be due to microbiological sulfate reduction and formation of ferro sulfides (Martens and Goldhaber 1978; Caraco et al. 1989). The release of Al and Fe oxide-bound P is dependent on pH (Hingston et al. 1967) and some oxide-bound P may be displaced as the result of elevated concentration of hydroxyl ions (OH^-). This may occur, for example, if resuspended particles containing Fe- or Al-bound P are mixed into a productive layer with higher pH than that in the near-bottom water (Drake and Heaney 1987). In addition, at higher pH, SiO_4–Si competes more efficiently with PO_4–P for sorption surfaces (Hingston et al. 1967).

Vertical and spatial distribution of P

The distribution of P fractions allows us to make inferences about the behaviour of P in the studied environment. In accordance with the low SAR value, the chemical character and the fairly uniform vertical distribution of sediment P at the mouth of the GoF (site 2) indicates a calm and relatively slow accumulation of P compounds (Fig. 3a, b). By comparison

Table 5 Total concentrations of dissolved elements extracted in NaBD and NaOH (steps I and II)

Depth (cm)	NaBD						NaOH					
	Mg	Si	Al	Ca	Mn	Fe	Mg	Si	Al	Ca	Mn	Fe
Site 1												
1	3.9	8.0	2.0	1.9	0.6	21.2	1.0	328	33.7	0.1	0	3.3
2	3.4	6.5	2.0	2.1	0.7	16.2	0.8	380	38.7	0	0.1	3.3
3	3.3	5.1	1.3	1.9	0.8	11.0	0.9	445	40.7	0	0.1	3.5
4	2.9	6.1	0.8	2.0	0.8	7.6	0	353	41.4	0	0	2.3
5	2.1	6.8	0.6	1.8	0.5	10.4	0.2	399	46.8	0	0	3.0
6	3.9	7.0	0.7	1.9	1.0	8.2	0.1	397	44.5	0	0	2.4
7	3.1	5.9	0.7	2.2	0.9	7.4	0	386	42.5	0	0	2.2
8	3.5	5.8	0.6	1.8	0.9	7.2	0	350	40.6	0	0	2.2
9	1.9	7.0	0.9	1.8	0.6	11.5	0.4	429	44.5	0	0.1	3.8
10	3.3	6.0	0.7	2.4	0.9	5.3	0.4	419	42.9	0	0.1	3.5
15	3.7	4.4	0.4	2.6	0.9	2.6	0.4	223	35.0	0	0.1	1.7
20	3.6	5.3	0.5	2.3	0.8	1.3	0.5	193	35.7	0	0.1	1.5
25	4.0	5.2	0.2	2.2	0.5	2.0	0.5	161	34.0	0	0	1.5
Site 2												
1	4.1	6.8	0.8	3.4	1.0	18.9	0.9	314	23.9	1.6	0.1	4.3
2	6.8	6.8	0.9	4.7	0.7	13.7	1.0	516	44.3	0.8	0.2	5.5
3	5.0	6.5	0.8	3.8	0.9	8.5	0.7	614	49.0	0	0.2	4.3
4	3.2	6.1	0.7	2.8	1.3	11.5	0.7	553	55.1	0	0.1	4.4
5	1.7	6.8	0.5	2.5	0.6	17.1	1.0	584	58.9	0.1	0.1	5.6
6	3.3	8.7	1.5	3.6	0.9	21.1	1.7	546	53.3	0	0.2	5.2
7	5.2	8.1	1.4	4.6	1.2	10.3	1.1	529	50.7	0	0.2	3.9
8	4.4	8.2	1.8	4.0	1.3	9.5	1.2	524	50.9	0	0.2	4.3
9	3.0	7.3	1.5	3.2	0.6	12.0	0.9	475	49.9	0	0.1	3.6
10	2.3	7.0	0.8	3.2	0.5	17.3	1.2	506	52.3	0	0.1	4.2
15	4.8	6.1	0.5	4.3	1.7	3.0	0.5	181	37.5	0	0.1	1.6
20	4.2	6.9	0.3	4.8	1.0	7.3	0.1	167	33.0	0	0	1.5
25	3.0	8.6	1.1	3.7	1.0	32.6	0.3	210	35.3	0	0.1	2.1
Site 3												
1	7.8	13.9	1.9	6.8	1.8	63.5	2.6	341	26.2	2.2	0.1	7.9
2	5.4	10.5	0.7	5.3	1.7	48.7	1.6	299	28.1	1.0	0	2.7
3	5.3	10.5	0.8	4.9	1.7	23.0	2.2	332	35.1	1.0	0	7.2
4	5.5	8.8	0.9	4.8	2.0	18.1	0.3	363	36.6	0.1	0.1	3.7
5	6.2	12.6	1.3	4.7	2.8	27.4	1.5	443	41.1	0.3	0.1	7.5
6	3.2	10.0	0.8	4.1	2.3	41.1	0.3	420	35.6	0	0.1	2.6
7	3.9	13.2	1.5	4.8	2.6	55.7	1.1	462	41.6	0.2	0.2	4.0
8	3.7	8.9	1.0	3.8	2.6	9.7	0.9	579	47.8	0	0.2	4.8
9	2.8	9.7	1.4	2.8	0.9	15.7	1.9	510	48.9	0	0.2	5.9
10	2.0	8.9	1.2	2.6	0.6	22.3	0.6	484	46.8	0	0.2	5.1
15	2.8	5.4	0.7	3.4	3.1	6.4	0.3	317	37.6	0	0.1	3.1
20	3.6	4.7	0.3	3.4	1.8	10.4	4.1	133	27.5	1.1	0.1	6.7
25	3.6	5.3	0.7	3.9	1.6	6.3	0.8	137	24.5	1.0	0.1	2.1

Table 5 continued

Depth (cm)	NaBD						NaOH					
	Mg	Si	Al	Ca	Mn	Fe	Mg	Si	Al	Ca	Mn	Fe
Site 4												
1	5.9	13.3	0.6	6.7	14.2	109	1.8	401	63.6	1.3	0.4	18.2
2	4.4	8.0	0.9	4.2	3.1	88.4	1.2	544	56.1	0.2	0.2	13.8
3	4.3	15.5	5.2	3.1	1.6	60.6	1.1	622	58.8	0	0.1	5.1
4	3.0	8.2	1.3	3.2	1.4	64.1	0	603	61.8	0	0.1	2.5
5	6.8	11.6	0.9	6.1	3.9	21.0	0.9	609	59.6	0.2	0.1	5.3
6	7.2	10.9	0.9	6.7	4.5	15.6	1.9	664	67.0	0.5	0.2	8.1
7	7.6	11.3	0.9	7.2	5.1	14.3	1.8	665	65.8	0.5	0.2	7.3
8	4.7	11.9	0.9	5.1	4.5	23.5	3.5	691	70.0	0.8	0.2	16.7
9	4.5	10.5	1.0	4.4	3.8	16.0	3.3	753	73.0	0.5	0.4	12.8
10	4.7	9.8	0.8	4.6	3.6	15.6	1.8	754	70.5	0.1	0.3	9.6
15	4.7	11.7	0.7	4.0	4.9	15.6	1.3	677	62.7	0.1	0.3	6.5
20	5.7	9.7	0.8	4.4	4.5	12.8	3.1	538	62.8	0.2	0.5	11.0
25	4.6	7.0	0.2	3.7	4.4	8.2	0.2	298	41.6	0	0.2	1.7
Site 5												
1	16.7	46.8	0.5	21.8	154	32.6	0.2	321	35.0	0.5	0.8	2.5
2	6.9	15.2	0.2	14.5	55.1	27.4	0.1	346	42.9	0.3	0.5	1.9
3	6.1	17.1	0.5	6.1	12.5	31.9	0	558	50.7	0	0.1	2.0
4	5.0	15.2	0.2	6.4	16.9	30.7	0.1	469	50.1	0	0.2	2.3
5	2.8	8.7	0.2	3.6	9.3	13.5	0.1	427	47.5	0	0.1	2.0
6	3.4	9.8	0	4.2	10.3	17.8	0.4	453	49.8	0	0.1	2.1
7	3.9	12.4	0	4.9	11.2	29.1	0.1	512	54.0	0	0.1	2.2
8	3.1	10.5	0	4.5	8.9	21.4	0.1	574	56.9	0	0.1	2.3
9	3.5	12.7	0	4.6	9.6	25.3	0	573	56.5	0	0.1	1.8
10	4.5	15.4	0	5.5	9.7	30.1	0	750	65.2	0	0.2	2.6
15	5.8	18.9	0.8	6.0	2.5	32.0	0.8	776	67.5	0.1	0.2	5.7
20	3.4	8.6	0.6	3.8	2.0	15.2	0	339	49.8	0.1	0.2	2.2
25	4.4	8.1	0.5	3.8	2.0	16.5	0	297	48.6	0	0.2	2.0
Site 6												
1	8.7	23.8	1.1	14.1	72.3	135	0	538	55.9	0	0.3	3.2
2	5.2	13.0	1.3	6.1	8.6	81.2	0.8	485	63.2	0	0.1	2.6
3	6.2	12.9	0.9	6.5	11.3	80.6	0.2	478	68.8	0.1	0.1	3.9
4	3.9	12.4	1.3	7.7	9.8	69.1	1.5	492	65.2	0.2	0.2	8.7
5	5.3	17.6	0.7	6.2	10.1	75.7	0.4	550	68.4	0.1	0.1	3.3
6	6.6	17.3	0.4	7.6	8.0	72.4	0.3	633	71.8	0	0.1	3.8
7	5.0	13.7	0.8	5.2	5.4	47.1	0.4	555	58.9	0.2	0.2	3.1
8	5.4	11.7	0.3	4.3	4.7	41.0	0.7	487	54.8	0	0.2	4.1
9	4.7	10.2	0.6	4.1	4.2	30.0	0.5	463	48.7	0.2	0.2	2.4
10	5.3	10.2	0.3	4.7	4.2	28.1	0.7	467	51.2	0	0.2	3.2
15	5.6	9.8	0.2	4.9	3.7	29.7	1.3	381	52.1	0.1	0.2	4.1
20	5.0	9.3	0.6	4.0	3.1	36.7	0.8	292	43.1	0	0.1	1.7
25	5.9	7.9	0.4	4.2	2.5	27.9	0.7	281	44.6	0	0.1	1.7

Table 5 continued

Depth (cm)	NaBD						NaOH					
	Mg	Si	Al	Ca	Mn	Fe	Mg	Si	Al	Ca	Mn	Fe
Site 7												
1	17.0	15.3	0.9	15.9	5.5	64.5	1.2	1,390	78.8	0.8	0.3	31.4
2	21.1	37.2	16.3	18.3	8.6	83.6	0.5	1,370	87.4	0.3	0.2	14.9
3	9.3	15.3	0.8	9.6	6.8	58.5	0.8	1,325	100	0.5	0.3	18.4
4	8.2	18.5	0.3	8.7	6.6	61.0	1.1	1,384	98.3	0.5	0.2	25.5
5	8.9	20.9	0.4	9.6	7.3	73.4	0.5	1,509	101	0.3	0.2	13.1
6	5.5	14.2	0.7	5.5	2.2	66.6	0.8	1,414	104	0.3	0.2	20.3
7	6.1	15.3	0.7	13.7	3.3	66.6	0.9	1,434	105	0.6	0.2	18.5
8	7.7	17.9	0.9	8.1	4.2	74.3	0	1,468	101	0	0.1	5.5
9	1.9	19.9	1.2	3.0	0.5	163	0	1,273	99.2	0.4	0.1	3.8
10	0.9	18.5	0.9	0.7	0.3	163	0	1,156	101	0.1	0.1	4.2
15	4.9	13.5	0.5	6.3	4.4	61.5	0	1,025	82.7	0.7	0.2	3.6

All concentrations are presented as μmol g^{-1} DW

0 Concentration below detection limit (<0.05 μmol g^{-1} DW)

Concentration differences (μmol P g^{-1} DW) for Mg, Si, Al, Ca, Mn, and Fe between triplicate or duplicate samples were the following (elements are listed in the same order): NaBD: <7.5, <30.9, <30.8, <4.5, <10.2, and <19.4; NaOH: <2.8, <144, <32.3, <1.2, <0.6, and <29.8

Table 6 Summary of significant correlations between different P fractions, sediment parameters, and other elements in extracts

Sed (as a subscript) = content in the sediment

All correlations were positive, except those with (−) sign

Dependent variable	Statistically significant correlation with
NaCl-iP	TMn_{sed}
NaBD-iP	TP_{sed}, NaCl-iP, NaBD-Fe, NaBD-Mn, NaBD-Si, NaOH-Ca, NaOH-Fe
NRP	TP_{sed}, Res-P, NaOH-iP
NaOH-iP	TMn_{sed}, Res-P, NRP, NaOH-Fe, NaOH-Mn, NaBD-Al
HCl-iP	TC_{sed} (−), Res-P
Res-P	TC_{sed}, TN_{sed}, TS_{sed}, TMn_{sed}, NaOH-iP, HCl-iP (−), NRP
Total organic P	TP_{sed}, TC_{sed}
TP_{extr}	TC_{sed}

the more uniform vertical distribution of P forms at northern Baltic Proper (site 1), with five times higher SAR than at site 2, suggests that the material at this site was well-mineralized before deposition or initially lower in OM than at site 2. At the two easternmost sites, on the other hand, sediment P strongly decreased with depth. This distribution pattern of sediment P may mainly result from the high OM and OP contents of the deposited material as well as its terrestrial origin and, thus, more refractory nature of OM than OM of marine origin. Moreover, at least occasionally increased dissolved O_2 content at these sites may have kept part of the OP bound to oxide surfaces (via PO_4-groups), which would slow their microbial degradation (Suzumura and Kamatani 1995; Celi et al. 1999). Almost all cores had traces of bioturbation below the sediment surface. This suggests that O_2 conditions were better in the past and that the vertical distribution of P has been affected by the activity of benthic animals.

Immobile P

The immobile P forms (NaOH-iP, HCl-iP, and Res-P) become buried and are removed from the nutrient cycle. Immobile P formed 34–81% of TP_{extr}. It was highest in the northern Baltic Proper (site 1) and dominated at the four westernmost sites and below

the surface layer in the central GoF. Immobile P was fairly uniform with depth and it became dominant when reactive P diminished.

The NaOH-iP fraction represents P strongly bound to oxide surfaces of metals not sensitive to reduction (Al oxides) (Psenner et al. 1984) and, as expected, this pool was uniform with sediment depth. This P fraction correlated positively with Al released in NaBD-extraction and to Fe and Mn that dissolved in NaOH (and TMn_{sed}; Table 6). Since the mechanism for P removal in this extraction step is replacement with OH^-, this finding suggests partial disruption of metal oxides (e.g. during dissolution of Fe in the previous step) and dissolution of aluminate and ferrate anions from mineral lattice edges. Alkaline extractant may also release elements from organo-metallic complexes (Gerke and Hermann 1992; Lopez 2004). The highest portion of P bound to oxides of non-reducible metals and the highest alkali-extractable Fe and Al at the easternmost site may be related to the location of site 7 near to the shore, i.e., related to the presence of terrestrial weathering products (e.g., Al oxyhydroxides) and to high OM content. Site 7 also had high alkali-extractable Si indicating the abundance of biogenic Si, which can result from presence of diatoms (Vallius 1999).

In agreement with earlier study in the southwestern Baltic (Jensen and Thamdrup 1993), the apatite-P (HCl-iP) was roughly uniform with depth, showing that it is relatively inert in sediment. However, in surface layers of the present OM-rich sediments, apatite-P always increased slightly with depth. This suggests the formation of some authigenic P mineral from refractory OP (Williams and Mayer 1972; Ruttenberg and Berner 1993; Delaney 1998), although the fractionation scheme we applied does not separate authigenic and detrital apatite-P (Ruttenberg 1992). Ruttenberg and Berner (1993) showed that authigenic apatite-P is formed also in shallow near shore sediments. In our poorly oxygenated sediments, apatite-P formed a large part of sediment P, especially in the northern Baltic Proper (site 1). Here, the deposited material probably had already lost its redox-sensitive and degradable P forms during transportation and settling. The portion of apatite-P was smaller in the OM- and OP-rich sediments in the inner bay. The statistically significant negative correlation between apatite-P and TC_{sed} and refractory OP may reflect this spatial difference.

The residual P fraction (Res-P) also reflected the increase in OM content towards the east. It is supposed to represent refractory OP (Ruttenberg 1992), as supported by its statistically significant positive correlation with TC_{sed}, TN_{sed}, and labile OP (i.e., NRP) (Table 6). However, it also contains some inorganic P (Ruttenberg 1992; Lopez 2004), possibly apatite-P and occluded P (Chang and Jackson 1957). The decrease of residual P with sediment depth, especially at the site highest in OM, indicates that the refractory OP fraction also contained some degradable P compounds. Relevant to this, Reitzel et al. (2007) proposed that, in lake sediments, part of the humic acids might become degraded in the long run. Another explanation for the decreasing trend could be increase in sedimentation (e.g. Kemp 1971) during the past years. Increase in the sedimentation has been reported in shallow coastal estuaries in the northern GoF (Vaalgamaa and Conley 2008) and in the Baltic Proper (Emeis et al. 2000). Although the refractory OP also includes slowly degrading OP compounds, changes in this fraction were not considered in P efflux estimates. Slight increase in apatite-P simultaneously with decrease in residual P may indicate sink-switching rather than release of P (Williams and Mayer 1972; Ruttenberg and Berner 1993; Delaney 1998; Ruttenberg 2005).

Reactive P

The reactive P forms (NaCl-iP, NaBD-iP, and NRP) are or may become transformed into available forms for algae and bacteria by biogeochemical processes. However, also reactive P forms are found in deep sediment layers (e.g. Jensen and Thamdrup 1993; Lukkari et al. 2008). Reactive P comprised 19–66% of TP_{extr} and it dominated in the topmost layer in the central basin and the inner Gulf as well as in some subsurface layers at the easternmost site (7). These P forms (excluding loosely bound P) were largely responsible for the decrease in TP_{sed} with sediment depth and, thus, for the release of sediment P, as also supported by the statistically significant positive correlation between labile OP and reductant-soluble P and TP_{sed} (Table 6).

Although soluble or loosely bound P (NaCl-iP) was only a minor portion of sediment TP_{extr}, it is important because of its direct availability for bacteria and algae (Van Eck 1982). Moreover, it was

highest in the fluffy surface sediment which is susceptible for resuspension. The presence of this P form indicates a lack of available sorption sites. This was in agreement with the statistically significant positive correlation between loosely bound P and the P fraction dependent on redox conditions (NaBD-iP) (Table 6) (see also Łukawska-Matuszewska and Bolałek 2008).

The Fe-bound P (NaBD-iP), being highest in the topmost sediment at the eastern sites with best O_2 conditions (Fig. 3a, b), indicated the ability of Fe oxyhydroxides to retain P. This interaction was supported by the statistically significant positive correlation between reductant-soluble P and Fe (and Mn) (Table 6). However, Fe–P was also abundant in surface sediment at the hypoxic central basin. Probably NO_3–N present in the near-bottom water allowed Fe to retain P (Mortimer 1941, 1971; Froelich et al. 1979). Even so, redox-dependent species did not always directly reflect O_2 and redox conditions, partly because of their short-term changes and the inaccuracy of measurements. Reductant-soluble P, Fe, and Mn were smallest at the two westernmost sites (Table 5) located in an area that has often suffered from hypoxia (FIMR, monitoring data). However, the Fe:P ratio in the reductant extract, assumed to indicate P retention ability of the sediment (Jensen and Thamdrup 1993; Coelho et al. 2004), was highest at the hypoxic site 4 (12.0) in the central GoF. Evidently at this site, the sediment surface has the potential to retain P if O_2 conditions improve. The low ratio at the neighboring site 5 (1.0), on the other hand, suggests that the sorption sites of the Fe oxides were more occupied with P than at the other sites. Earlier studies in the Baltic have reported the reduction induced decrease in Fe–P with sediment depth (Jensen and Thamdrup 1993; Carman 1998; Aigars 2001; Łukawska-Matuszewska and Bolałek 2008; Lukkari et al. 2008, 2009). Nevertheless, the reductant also dissolves Fe not active in P binding (Mehra and Jackson 1960; Jensen and Thamdrup 1993). In fact, in this study, some reductant-soluble P and Fe were found in the deep layers of open sea sediments (mostly at the site closest to the shore), though clearly less than in the deep layers of estuaries (Lukkari et al. 2008). This indicates more efficient ferric-iron removal via sulfate reduction and ferro sulfide formation in open sea sediments than in estuary sediments, as suggested by Hyacinthe and Van Cappellen (2004). Berner et al. (1993) and Slomp et al. (1996) suggested that incomplete Fe reduction would result in the burial of Fe–P.

Labile OP (NRP) was the dominating P form at the easternmost site (7), coinciding with high OC and OP. The decreasing trend of this fraction with sediment depth indicates degradation of OP, though the fraction also contains slowly degradable compounds and transformation products. Reitzel et al. (2006) identified pyrophosphate, polyphosphate, and orthophosphate mono- and diesters in the NRP fraction. Slightly oxic conditions at site 7 may have favored microbial synthesis of polyphosphates (Ingall and Jahnke 1994; Hupfer et al. 1995). Ahlgren et al. (2006) estimated that the half-life ($T_{½}$) of organic and biogenic P compounds varied from 3 to 16 years in anoxic Baltic Sea sediments. At our sampling sites, however, $T_{½}$ of the whole labile OP fraction (determined by exponential fitting of concentrations vs. sediment age, $R^2 > 0.6$, assuming constant SAR), varied from 18 to 66 years. The longer $T_{½}$ for the whole fraction than for separate compounds may be due to the presence of unidentified compounds. Also, the origin of OP seems to be relevant, as $T_{½}$ was longest at the mouth of the Gulf and shortest at the easternmost site, closest to high P loading.

The down-core decreasing trend of labile and refractory OP in open sea sediments was different from what we found in estuaries (Lukkari et al. 2008). This difference suggests that a larger portion of OP degrades in the surface of poorly oxygenated open sea sediments than in shallow estuaries. The better O_2 conditions in estuaries, which favor the retention of OP compounds onto oxide surfaces with a binding mechanism similar to that of PO_4–P, retard the degradation of OP (Suzumura and Kamatani 1995; Celi et al. 1999). In agreement with this, Virtasalo et al. (2005) concluded from the higher organic C:P ratios that, in the Archipelago Sea, OP release was higher in the anoxic sediments than in the oxic and suboxic sediments. Similarly, Edlund and Carman (2001) reported a higher sediment organic C:P ratio in anoxic than in oxic areas in the Baltic. These findings are in accordance with the enhanced release of OP under O_2 depletion reported by Ingall et al. (1993).

As in the main basins of the Baltic (Carman 1998), the sediment C:N ratio in the GoF (range 9.4–12.6) was fairly uniform spatially and vertically. In agreement with previous studies in the Baltic (Carman

1998; Emeis et al. 2000; Edlund and Carman 2001), the C:N ratio exceeded the Redfield ratio (Redfield et al. 1963) in all samples, indicating enrichment of the sediment with C. Thus, N compounds may have been preferentially degraded in the early stages of diagenesis (Krom and Berner 1981), or OM may have contained terrestrial OM with higher C:N ratios than marine OM (Ruttenberg and Goñi 1997; Carman 1998; Ruttenberg 2005). Also, the organic C:P ratio exceeded the Redfield ratio, probably for the same reasons as the C:N ratio did (Krom and Berner 1981; Froelich et al. 1982, Froelich et al. 1979; Berner et al. 1993), though the OC:OP ratio (range 154–289) was more variable than the C:N ratio. Furthermore, although TC_{sed} increased eastwards in the GoF, the organic C:P ratio decreased (Fig. 6). Evidently, OP increased faster towards the inner GoF, as would be expected from the high P load from the River Neva (HELCOM 2003).

Sampling season may have affected the OM content of the sediments. Aigars (2001) found decrease in inorganic P at the sediment surface during late summer in the Gulf of Riga. In the GoF, the difference in the P fractions between spring and autumn was studied at sites 5 and 6 (Lukkari 2008). The differences mainly occurred in the topmost 1–2 cm layer: Fe–P was lower, while labile OP (and loosely bound P) was higher in autumn than in spring. The results can reflect the increased OM, and O_2 consumption, at the surface during the summer. Thus, surface sediments at sites 4, 5, and 6 may be lower in OP than the rest of the sites partly because they were sampled in spring.

Dissolved species at the sediment–water interface

The dissolved species at the sediment–water interface reflect the dynamic biogeochemical processes affecting the behaviour of sediment P and the prevailing conditions. The highest incubation-derived PO_4–P flux out from the sediment (Table 2) at the OM-rich easternmost site (7) and at the most hypoxic site (3) in the central GoF co-occurred with a steep PO_4–P concentration gradient at the sediment–water interface (Fig. 2). In contrast to this, at the slightly oxic site 6, the PO_4–P gradient was smooth and the incubation-derived PO_4–P flux was negative. It is noteworthy that at site 7 the PO_4–P flux was highly positive despite the slightly oxic near-bottom water and high NO_3–N at the sediment–water interface. At this site, the sediment surface was high in TC_{sed} and OP, and part of PO_4–P probably originated in the mineralized OP pool. The fairly high NH_4–N, evidently, released from OM to the near-bottom water, supported this conclusion (Martens and Goldhaber 1978; Kamp-Nielsen 1992; Lukkari et al. 2009). Both O_2 and NO_3–N were present, and ferric (Fe^{3+}) oxyhydroxides should therefore have kept PO_4–P in adsorbed form. However, redox conditions (Fig. 5) at the sediment–water interface ($E_h < 230$ mV; Mortimer 1941) suggest that reduction of Fe^{3+} had taken place. In fact, the near-bottom water was high in Fe_{diss} while the pore water in the surface sediment was low in Fe_{diss}. This implies that the ability of sediment to retain P was low, and mineralization-derived P was released. Incubation-derived PO_4–P flux at the easternmost site (7) was higher than determined earlier in the GoF by Conley et al. (1997) and Lukkari et al. (2009). However, e.g., Val Klump and Martens (1981) reported even higher PO_4–P flux in OM-rich, anoxic Cape Lookout Bight (USA) than in the poorly oxygenated sediments in the open GoF.

In general, the relatively low pore water Fe_{diss} (Figs. 2, 3b) can be attributed to the escape of Fe_{diss} to the water column or its precipitation as ferric oxyhydroxides in oxic conditions or as ferrous sulfides in anoxic conditions (Mortimer 1941, 1971; Berner 1970; Froelich et al. 1979; Krom and Berner 1980). Site 6 was an exception: pore water Fe_{diss} exhibited a gradient in the sediment–water interface (Fig. 2). As Fe_{diss} in the near-bottom water was relatively low, we conclude that the O_2 concentration (2.4 ml l^{-1}) was high enough for precipitation of Fe oxyhydroxide. This conclusion was supported by the high reductant-soluble Fe and P in the surface sediment (Table 5; Fig. 3b). The chemistry of Mn provides further information about conditions at the sediment–water interface (Figs. 2, 3b). At the three westernmost sites (1, 2, and 3), both Mn_{diss} and reductant-soluble Mn were low at the sediment surface because the easily reducible Mn (e.g. Mortimer 1971) had diffused out from the sediment. At sites 4, 5, and 6, in contrast, pore water Mn_{diss}, (Fig. 2), TMn_{sed} peak values (Table 3), and abundant reductant-soluble Mn in the topmost layer (Table 5) suggest that part of the Mn was precipitated as oxides (Froelich et al. 1979), possibly participating in P binding.

Burial and potential for release of sediment P along the west-to-east transect

Immobile and reactive P forms can be used in evaluating the burial and potential for release of P from the sediment reserves. Because reactive P forms are also present in deep sediment layers, their buried concentrations are taken into account in calculations of the burial flux of P. Thus, only the remainder of the reactive P at the surface represents potentially mobile P, which is prone to release from sediment with time (Lukkari et al. 2008). Since SAR varied among the sites, the known depth layer, from the year 1986, was chosen as background for buried reactive P at each site.

Although the central basin of the GoF (site 5) had highest sedimentation and burial of P (Table 4), it also had highest P efflux (i.e., the long-term average of minimum annual P release calculated from the solid phase P data), because the burial efficiency for total P in the surface sediment was only 63%. The three westernmost sites had lower P efflux than the other sites. The low P efflux at the mouth of the GoF (site 2) is explained by the smaller P sedimentation, but that in the northern Baltic Proper (site 1) is apparently due to the apatitic nature and, thus, high burial efficiency of sediment P. The difference in P burial at the two easternmost sites seems to be due to the different composition of reactive P. The dominant form at site 6 was Fe–P and most of this will be released by reduction in subsurface layers (e.g. Williams et al. 1976), while the dominant form at site 7 was labile OP, which will be partly (slowly) degraded. In both cases, however, release of P is affected by O_2 conditions.

P fractionation results suggest that, on average, the studied poorly oxygenated sediments will bury 74% of the total P at the sediment surface and the rest will be released back to the water column in the long run. In the central basin and at site 6, however, the abundant redox-dependent P at the surface (Fig. 3a, b) creates the potential for P release in relatively short time scale (e.g. Hietanen and Lukkari 2007). In general, sedimentation (and burial) of P in these open sea sediments was lower than that in two estuaries in the same region (Lukkari et al. 2008), but it was the same order of magnitude as reported, for example, in Aarhus Bay (Jensen et al. 1995), Kiel Bight (Balzer 1986), and Gotland Basin (Struck et al. 2004) in the Baltic. In the central and eastern GoF, burial flux of P was higher than for example in the Gulf of St. Lawrence (Louchouarn et al. 1997), but at the mouth of the Gulf it was close to that reported by Ingall and Jahnke (1994) in Peru margin and in Santa Monica Basin. Using the sediment dating information (^{137}Cs maxima in 1986), we can evaluate the amount of reactive P lost between 1986 and the sampling year. Assuming that (1) all reactive P lost was released from the sediment to water, (2) the SAR was constant, and (3) the composition of deposited material was more or less constant, we can roughly estimate that the long-term average of minimum annual P release from sediment reserves in open sea area ranged from 1.3 (at the mouth of the GoF) to 46.0 (in the central GoF) kg P km^{-2} (Table 4). Furthermore, excluding the site in the northern Baltic Proper, we can roughly estimate that in the GoF, poorly oxygenated bottom areas (with water depth ca. >60 m) have released, on average, at the minimum 19 kg P km^{-2} per year during the 17–18 year period after 1986. Note, however, that this estimation involves assumptions and considers only information stored in the sediment; it does not take into account the temporarily pronounced P release from particulate material during or immediately after deposition, e.g., settling of algal blooms. In fact, P efflux calculated on the basis of P fractions (Table 4) was not comparable with incubation-derived PO_4–P flux determinations (Table 2). This is not surprising, as the former represents a long-term average result of biogeochemical processes, while the latter represents a temporary situation (Krom and Berner 1981). Furthermore, O_2 conditions in the GoF deteriorated in the late 1990s, as reflected in the elevated PO_4–P concentrations in the water (Olsonen 2007) and intense algal blooms. Thus, the P efflux based on solid phase data probably overestimates the efflux during good O_2 conditions and underestimates that during hypoxia.

Conclusions

Sediment P concentration increased along a continuum from the northern Baltic Proper (west) to the inner GoF (east), and the chemical composition and vertical distribution of P reserves changed with changing sediment properties. Concentration of OM, which increased eastwards (i.e., towards the highest P loading) seemed to be the main determinant of the

chemical character of P. As a general trend, OP was abundant and increased towards the inner bay, while apatite-P decreased. Loosely bound P was relatively small, and the portion of Al-bound P relative to total P was fairly stable. Because of the poor O_2 conditions in the present open sea sediments during sampling, Fe-bound P was relatively low, which emphasized the role of OP in P release. However, Fe–P was present in the surface sediments in the central basin of the GoF despite the low concentration of dissolved O_2 in the near bottom water. The chemistry of dissolved Fe and Mn as well as P and N species at the sediment–water interface suggests fluctuating redox conditions with dissolution and precipitation reactions in the central and eastern GoF. Thus, we suggest that in this kind of environment, long-term information on P release derived from solid phase P data can support valuable minimum estimates of sediment P release. Study of sediment P release by incubation-derived flux determinations would require repeated determinations during the year, preferentially carried out in situ, to avoid errors arising from short-term changes in redox conditions.

This study showed that variation in the chemical composition of sediment P can have a marked effect on its release also in poorly oxygenated sediments, i.e., in conditions where the role of redox-sensitive Fe-bound P is less important than in oxic sediments. Furthermore, our results suggest that despite the considerable portion of OP that seems to be buried with sediment in the GoF, part of it is degradable. The abundance of labile OP increased towards inner bay and the high P loading. Since the portion of OP of total P is high, especially in the eastern GoF, it may be an important source for slow but more or less continuous P release from the sediment. Release is more pronounced if poor O_2 conditions hinder the formation at the sediment surface of Fe oxyhydroxides, which can trap upwards diffusing mineralization-released P. The high OP content and relatively slow degradation rate of some OP compounds in sediments may partly explain the slow response of the GoF to decreased anthropogenic P loading.

Acknowledgments Financial support was received from the Ministry of the Environment, the Kone Foundation, the Finnish Institute of Marine Research (FIMR), and the Maj and Tor Nessling Foundation. We thank the technicians from the FIMR for help in the P fractionation, and the laboratory for Environmental Research, University of Jyväskylä, for the metal determinations. We are indebted to Henry Vallius, Jyrki Hämäläinen, Kimmo Alvi, and Boris Winterhalter from GTK for help in sediment descriptions and echo sounding during cruises of r/v Aranda, and to Kalervo Mäkelä and Hannu Haahti (FIMR) for the pore water data in the sediment–water interface and the incubation-derived nutrient flux measurements. We thank the personnel of r/v Aranda for assistance during cruises and Helinä Hartikainen for valuable comments on the manuscript. Advice on the statistical analysis was received from Ville Hallikainen, Risto Häkkinen, Jaakko Heinonen, and Juha Hyvönen from the Finnish Forest Research Institute. This study was part of a project within the SEGUE consortium (Searching for protection tools for the eutrophied GoF—Integrated use of research and modelling tools) carried out in collaboration with the University of Helsinki and the Finnish Environment Institute. SEGUE was part of the Baltic Sea Research Programme by the Academy of Finland.

References

Ahlgren J, Reitzel K, Tranvik L, Gogoll A, Rydin E (2006) Degradation of organic phosphorus compounds in anoxic Baltic Sea sediments: a ^{31}P nuclear magnetic resonance study. Limnol Oceanogr 51(5):2341–2348

Aigars J (2001) Seasonal variations in phosphorus species in the surface sediments of the Gulf of Riga, Baltic Sea. Chemosphere 45:827–834

Alenius P, Myrberg K, Nekrasov A (1998) The physical oceanography of the Gulf of Finland: a review. Boreal Environ Res 3(2):97–125

Anschutz P, Zhong S, Sundby B, Mucci A, Gobeil C (1998) Burial efficiency of phosphorus and the geochemistry of iron in continental margin sediments. Limnol Oceanogr 43(1):53–64

Balzer W (1986) Forms of phosphorus and its accumulation in coastal sediments of Kieler Bucht. Ophelia 26:19–35

Bender M, Martin W, Hess J, Sayles F, Ball L, Lambert C (1987) A whole-core squeezer for interfacial pore-water sampling. Limnol Oceanogr 32(6):1214–1225

Berner RA (1970) Sedimentary pyrite formation. Am J Sci 268:1–23

Berner RA, Ruttenberg KC, Ingall ED, Rao J-L (1993) The nature of phosphorus burial in modern marine sediments. In: Wollast R, Mackenzie FT, Chou L (eds) Interactions of C, N, P and S Biogeochemical Cycles and Global Change. NATO ASI Series, 14. Springer, Berlin, pp 365–378

Boström B, Jansson M, Forsberg C (1982) Phosphorus release from lake sediments. Arch Hydrobiol Beih Ergebn Limnol 18:5–59

Caraco NF, Cole JJ, Likens GE (1989) Evidence for sulphate-controlled phosphorus release from sediments of aquatic systems. Nature 341:316–318

Carman R (1998) Burial pattern of carbon, nitrogen and phosphorus in the soft bottom sediments of the Baltic Sea. Vie Milieu 48(4):229–241

Carman R, Jonsson P (1991) Distribution patterns of different forms of phosphorus in some surficial sediments of the Baltic Sea. Chem Geol 90:91–106

Celi L, Lamacchia S, Marsan FA, Barberis E (1999) Interaction of inositol hexaphosphate on clays: adsorption and charging phenomena. Soil Sci 164(8):574–585

Chang SC, Jackson ML (1957) Fractionation of soil phosphorus. Soil Sci 84:133–144

Coelho JP, Flindt MR, Jensen HS, Lillebø AI, Pardal MA (2004) Phosphorus speciation and availability in intertidal sediments of a temperate estuary: relation to eutrophication and annual P-fluxes. Estuar Coast Shelf Sci 61: 583–590

Conley DJ, Stockenberg A, Carman R, Johnstone RW, Rahm L, Wulff F (1997) Sediment-water nutrient fluxes in the Gulf of Finland, Baltic Sea. Estuar Coast Shelf Sci 45:591–598

Delaney ML (1998) Phosphorus accumulation in marine sediments and the oceanic phosphorus cycle. Glob Biogeochem Cycles 12(4):563–572

Drake JC, Heaney SI (1987) Occurrence of phosphorus and its potential remobilization in the littoral sediments of a productive English lake. Freshwat Biol 17:513–523

Drever JI (2002) The geochemistry of natural waters. Surface and groundwater environments, 3rd edn. Prentice Hall, New Jersey, p 436

Eckert JM, Sholkovitz ER (1976) The flocculation of iron, aluminium and humates from river water by electrolytes. Geochim Cosmochim Acta 40:847–848

Edlund G, Carman R (2001) Distribution and diagenesis of organic and inorganic phosphorus in sediments of the Baltic proper. Chemosphere 45:1053–1061

Einsele W (1936) Über die Beziehungen des Eisenkreislaufs zum Phophatkreislauf im eutrophen See. Arch Hydrobiol 29:664–686

Einsele W (1938) Über chemische und kolloidchemische Vorgänge in Eisen-Phosphat-Systemen unter limnochemischen und limnogeologischen Gesichtspunkten. Arch Hydrobiol Plankt 33:361–387

Emeis K-C, Struck U, Leipe T, Pollehne F, Kunzendorf H, Christiansen C (2000) Changes in the C, N, P burial rates in some Baltic Sea sediments over the last 150 years–relevance to P regeneration rates and the phosphorus cycle. Mar Geol 167:43–59

Froelich PN, Klinkhammer GP, Bender ML, Luedtke NA, Heath GR, Cullen D, Dauphin P, Hammond D, Hartman B (1979) Early oxidation of organic matter in pelagic sediments of the eastern equatorial Atlantic: suboxic diagenensis. Geochim Cosmochim Acta 43:1075–1090

Froelich PN, Bender ML, Luedtke NA, Heath GR, DeVries T (1982) The marine phosphorus cycle. Am J Sci 282: 474–511

Gerke J, Hermann R (1992) Adsorption of orthophosphate to humic-Fe-complexes and to amorphous Fe-oxide. Z Pflanzenernähr Bodenk 155:233–236

Grasshoff K (1983) Determination of oxygen. In: Grasshoff K, Ehrhardt M, Kremling K (eds) Methods of seawater analysis, 2nd edn. Verlag Chemie Gmbh, Weinheim, pp 61–72

Hansen HP, Koroleff F (1999) Determination of nutrients. In: Grasshoff K, Kremling K, Ehrhardt M (eds) Methods of seawater analysis, 3rd edn. Wiley-VCH Verlag Chemie Gmbh, Weinheim, pp 159–228

HELCOM (2003) The Baltic Marine Environment 1999–2002. Baltic Sea Environment Proceedings No. 87. Erweko Painotuote Oy, Helsinki, p 47

Hietanen S, Lukkari K (2007) Effects of short-term anoxia on benthic denitrification, nutrient fluxes and phosphorus forms in coastal Baltic sediment. Aquatic Microb Ecol 49:293–302

Hingston FJ, Atkinson RJ, Posner AM, Quirk JP (1967) Specific adsorption of anions. Nature 215:1459–1461

Hupfer M, Gächter R, Rüegger H (1995) Polyphosphate in lake sediments: ^{31}P NMR spectroscopy as a tool for its identification. Limnol Oceanogr 40(3):610–617

Hyacinthe C, Van Cappellen P (2004) An authigenic iron phosphate phase in estuarine sediments: composition, formation and chemical reactivity. Mar Chem 91:227–251

Ingall E, Clark L (1998) Redox-dependent phosphorus cycling: microbial and abiotic processes. Mineral Mag 62A: 677–678. doi:10.1180/minmag.1998.62A.2.23

Ingall E, Jahnke R (1994) Evidence for enhanced phosphorus regeneration from marine sediments overlain by oxygen depleted waters. Geochim Cosmochim Acta 58(11): 2571–2575

Ingall ED, Bustin RM, Van Cappellen P (1993) Influence of water column anoxia on the burial and preservation of carbon and phosphorus in marine shales. Geochim Cosmochim Acta 57:303–316

Ingri J, Löfvendahl R, Boström K (1991) Chemistry of suspended particles in the southern Baltic Sea. Mar Chem 32:73–87

Jensen HS, Thamdrup B (1993) Iron-bound phosphorus in marine sediments as measured by bicarbonate-dithionite extraction. Hydrobiologia 253:47–59

Jensen HS, Mortensen PB, Andersen FØ, Rasmussen E, Jensen A (1995) Phosphorus cycling in a coastal marine sediment, Aarhus Bay, Denmark. Limnol Oceanogr 40(5): 908–917

Jørgensen BB (1977) The sulfur cycle of a coastal marine sediment (Limfjorden, Denmark). Limnol Oceanogr 22(5): 814–832

Kamp-Nielsen L (1992) Benthic-pelagic coupling of nutrient metabolism along an estuarine eutrophication gradient. Hydrobiologia 235/236:457–470

Kankaanpää H, Vallius H, Sandman O, Niemistö L (1997) Determination of recent sedimentation in the Gulf of Finland using 137-Cs. Oceanol Acta 20(6):823–836

Kemp ALW (1971) Organic carbon and nitrogen in the surface sediments of Lakes Ontario, Erie and Huron. J Sediment Petrol 41(2):537–548

Klump JV, Martens CS (1981) Biogeochemical cycling in an organic-rich coastal marine basin–II. Nutrient sediment-water exchange processes. Geochim Cosmochim Acta 45:101–121

Koistinen T, Stephens MB, Bogatchev V, Norgulen Ø, Wennerström M, Korhonen J (2001) Geological map of the Fennoscandian Shield, scale 1:2 000 000. Geological Surveys of Finland, Norway and Sweden and Ministry of Natural Resources of Russia. Espoo, Trondheim, Uppsala, Moscow

Koroleff F (1983) Determination of phosphorus. In: Grasshoff K, Ehrhardt M, Kremling K (eds) Methods of seawater

analysis, 2nd edn. Verlag Chemie Gmbh, Weinheim, pp 125–142

Kotilainen A, Vallius H, Ryabchuk D (2007) Seafloor anoxia and modern laminated sediments in coastal basins of the Eastern Gulf of Finland, Baltic Sea. In: Holocene sedimentary environment and sediment geochemistry of the eastern Gulf of Finland, Baltic Sea. Geological Survey of Finland, 45, Espoo, pp 49–62

Krom MD, Berner RA (1980) Adsorption of phosphate in anoxic marine sediments. Limnol Oceanogr 25(5):797–806

Krom MD, Berner RA (1981) The diagenesis of phosphorus in a nearshore marine sediment. Geochim Cosmochim Acta 45:207–216

Kullenberg G (1981) Physical oceanography. In: Vopio A (ed) The Baltic Sea. Elsevier oceanography series 30, Netherlands, pp 135–181

Kyzyurov V, Mikheev Y, Niemistö L, Winterhalter B, Häsänen E, Ilus E (1994) Shipboard determination of deposition rates of recent sediments based on Chernobyl derived Cesium-137. Baltica 8:64–67

Lehtoranta J (1998) Net sedimentation and sediment-water nutrient fluxes in the eastern Gulf of Finland (Baltic Sea). Vie et Milieu 48(4):341–352

Leivuori M (2000) Distribution and accumulation of metals in sediments of the northern Baltic Sea. Finnish Institute of Marine Research—Contributions, No 2. Dissertation, University of Helsinki

Lopez P (2004) Spatial distribution of sedimentary P pools in a Mediterranean coastal lagoon 'Albufera d'es Grau' (Minorca Island, Spain). Mar Geol 203:161–176

Loring DH, Rantala RTT (1992) Manual for the geochemical analyses of marine sediments and suspended particulate matter. Earth Sci Rev 32:235–283

Louchouarn P, Lucotte M, Duchemin E, de Vernal A (1997) Early diagenetic processes in recent sediments of the Gulf of St-Lawrence: phosphorus, carbon and iron burial rates. Mar Geol 139:181–200

Łukawska-Matuszewska K, Bolałek J (2008) Spatial distribution of phosphorus forms in sediments in the Gulf of Gdańsk (southern Baltic Sea). Cont Shelf Res 28(7): 977–990

Lukkari K (2008) Chemical characteristics and behaviour of sediment phosphorus in the northeastern Baltic Sea. Finnish Institute of Marine Research—Contributions, No 17. Dissertation, University of Helsinki

Lukkari K, Leivuori M, Hartikainen H (2007a) Fractionation of sediment phosphorus revisited. II: changes in phosphorus fractions during sampling and storing in the presence or absence of oxygen. Limnol Oceanogr Meth 5:445–456

Lukkari K, Hartikainen H, Leivuori M (2007b) Fractionation of sediment phosphorus revisited. I: fractionation steps and their biogeochemical basis. Limnol Oceanogr Meth 5:433–444

Lukkari K, Leivuori M, Hartikainen H (2008) Vertical distribution and chemical character of sediment phosphorus in two shallow estuaries in the Baltic Sea. Biogeochem 90(2):171–191

Lukkari K, Leivuori M, Vallius H, Kotilainen A (2009) The chemical character and burial of phosphorus in shallow coastal sediments in the northeastern Baltic Sea. Biogeochem 94(2):141–162

Mäkelä K, Tuominen L (2003) Pore water nutrient profiles and dynamics in soft bottoms of the northern Baltic Sea. Hydrobiologia 492:43–53

Martens CS, Goldhaber MB (1978) Early diagenesis in transitional sedimentary environments of the White Oak River Estuary, North Carolina. Limnol Oceanogr 23(3):428–441

Mattila J, Kankaanpää H, Ilus E (2006) Estimation of recent sediment accumulation rates in the Baltic Sea using artificial radionuclides 137Cs and 239, 240Pu as time markers. Boreal Environ Res 11:95–107

Mehra OP, Jackson ML (1960) Iron oxide removal from soils and clays by a dithionite-citrate system buffered with sodium bicarbonate. Clays Clay Miner 7:317–327

Mortimer CH (1941) The exchange of dissolved substances between mud and water in lakes, I. J Ecol 29:280–329

Mortimer CH (1942) The exchange of dissolved substances between mud and water in lakes, II. J Ecol 30:147–201

Mortimer CH (1971) Chemical exchanges between sediments and water in the Great Lakes–speculations on probable regulatory mechanisms. Limnol Oceanogr 16(2):387–404

Neretin LN, Pohl C, Jost G, Leipe T, Pollehne F (2003) Manganese cycling in the Gotland Deep, Baltic Sea. Mar Chem 82:125–143

Olsonen R (ed) (2007) FIMR Monitoring of the Baltic Sea Environment—annual report 2006. Meri, Report Series of the Finnish Institute of Marine Research, 59, p 58

Perttilä M, Niemistö L, Mäkelä K (1995) Distribution, development and total amounts of nutrients in the Gulf of Finland. Estuar Coast Shelf Sci 41:345–360

Pettersson K, Boström B, Jacobsen O-S (1988) Phosphorus in sediments–speciation and analysis. Hydrobiologia 170: 91–101

Psenner R, Pucsko R, Sager M (1984) Die Fraktionierung organischer und anorganischer Phosphorverbindungen von Sedimenten. Versuch einer Definition ökologisch wichtiger Fraktionen. Fractionation of organic and inorganic phosphorus compounds in lake sediments. An attempt to characterize ecologically important fractions. Arch Hydrobiol/Suppl 70:111–155

Redfield AC, Ketchum BH, Richards FA (1963) The influence of organisms on the composition of sea-water. In: Hill MN (ed) The sea: ideas and observations on progress in the study of the seas. The composition of sea-water: comparative and descriptive oceanography, vol 2, Interscience Publishers, New York, pp 26–77

Reitzel K, Ahlgren J, Gogoll A, Jensen HS, Rydin E (2006) Characterization of phosphorus in sequential extracts from lake sediments using ^{31}P nuclear magnetic resonance spectroscopy. Can J Fish Aquat Sci 63:1686–1699

Reitzel K, Ahlgren J, DeBrabandere H, Waldebäck M, Gogoll A, Tranvik L, Rydin E (2007) Degradation rates of organic phosphorus in lake sediment. Biogeochem 82: 15–28

Ruban V, López-Sánchez JF, Pardo P, Rauret G, Muntau H, Quevauviller PH (1999) Selection and evaluation of sequential extraction procedures for the determination of phosphorus forms in lake sediment. J Environ Monit 1:51–56

Ruttenberg KC (1992) Development of a sequential extraction method for different forms of phosphorus in marine sediments. Limnol Oceanogr 37(7):1460–1482

Ruttenberg KC (2005) The global phosphorus cycle. In: Schlesinger WH (ed) Biogeochemistry. Holland HD, Turekian KK (eds) Treatise on geochemistry, Elsevier, Italy, vol 8, pp 585–644

Ruttenberg KC, Berner RA (1993) Authigenic apatite formation and burial in sediments from non-upwelling, continental margin environments. Geochim Cosmochim Acta 57:991–1007

Ruttenberg KC, Goñi MA (1997) Depth trends in phosphorus distribution and C:N:P ratios of organic matter in Amazon Fan sediments: indices of organic matter source and burial history. In: Flood RD, Piper DJW, Klaus A, Peterson LC (eds) Proceedings of the ocean drilling program, Scientific Results, vol 155, pp 505–517

Ryden JC, Syers JK, Tillman RW (1987) Inorganic anion sorption and interactions with phosphate sorption by hydrous ferric oxide gel. J Soil Sci 38:211–217

Schnitzer M (1969) Reactions between fulvic acid, a soil humic compound and inorganic soil constituents. Soil Sci Soc Amer Proc 33:75–81

Sholkovitz ER (1976) Flocculation of dissolved organic and inorganic matter during the mixing of river water and seawater. Geochim Cosmochim Acta 40:831–845

Slomp CP, Van der Gaast SJ, Van Raaphorst W (1996) Phosphorus binding by poorly crystalline iron oxides in North Sea sediments. Mar Chem 52:55–73

Smith RL, Klug MJ (1981) Reduction of sulfur compounds in the sediments of a eutrophic lake basin. Appl Environ Microbiol 41(5):1230–1237

Struck U, Pollehne F, Bauerfeind EV, Bodungen B (2004) Sources of nitrogen for the vertical particle flux in the Gotland Sea (Baltic Proper)–results from sediment trap studies. J Mar Syst 45:91–101

Stumm W, Morgan JJ (1996) Aquatic chemistry. Chemical equilibria and rates in natural waters, 3rd edn. John Wiley & Sons, New York, p 1022

Sundby B, Gobeil C, Silverberg N, Mucci A (1992) The phosphorus cycke in coastal marine sediments. Limnol Oceanogr 37(6):1129–1145

Suzumura M, Kamatani A (1995) Mineralization of inositol hexaphosphate in aerobic and anaerobic marine sediments: implications for the phosphorus cycle. Geochim Cosmochim Acta 59(5):1021–1026

Vaalgamaa S, Conley DJ (2008) Detecting environmental change in estuaries: nutrient and heavy-metal distributions in sediment cores in estuaries from the Gulf of Finland, Baltic Sea. Estuar Coast Shelf Sci 76:45–56

Vallius H (1999) Recent sediments of the Gulf of Finland: an environment affected by the accumulation of heavy metals. Dissertation, Åbo Akademi University, p 43

Vallius H (2006) Permanent seafloor anoxia in coastal basins of the northwestern Gulf of Finland, Baltic Sea. Ambio 35(3):105–108

Van Eck GTM (1982) Forms of phosphorus in particulate matter from the Hollands Diep/Haringvliet, The Netherlands. Hydrobiologia 92:665–681

Virtasalo JJ, Kotilainen AT (2008) Phosphorus forms and reactive iron in lateglacial, postglacial and brackish-water sediments of the Archipelago Sea, northern Baltic Sea. Marine Geology 252(1–2):1–12

Virtasalo JJ, Kohonen T, Vuorinen I, Huttula T (2005) Sea bottom anoxia in the Archipelago Sea, northern Baltic Sea - Implications for phosphorus remineralization at the sediment surface. Mar Geol 224:103–122

Williams JDH, Mayer T (1972) Effects of sediment diagenesis and regeneration of phosphorus with special reference to Lakes Erie and Ontario. In: Allen HE, Kramer JP (eds) Nutrients in natural waters. Wiley & Sons, New York, pp 281–315

Williams JDH, Syers JK, Armstrong DE, Harris RF (1971) Characterization of inorganic phosphate in noncalcareous lake sediments. Soil Sci Soc Amer Proc 35:556–561

Williams JDH, Jaquet J-M, Thomas RL (1976) Forms of phosphorus in the surficial sediments of Lake Erie. J Fisher Res Board Can 33(3):413–429

Winterhalter B, Flodén T, Ignatius H, Axberg S, Niemistö L (1981) Geology of the Baltic Sea. In: Vopio A (ed) The Baltic Sea. Elsevier oceanography series, 30, Netherlands, pp 1–121